



Cycle-Star Motifs: Network Response to Link Modifications

Sajjad Bakrani^{1,2} · Narcicegi Kiran^{1,2} · Deniz Eroglu¹ · Tiago Pereira^{2,3}

Received: 10 July 2022 / Accepted: 20 March 2024
© The Author(s) 2024

Abstract

Understanding efficient modifications to improve network functionality is a fundamental problem of scientific and industrial interest. We study the response of network dynamics against link modifications on a weakly connected directed graph consisting of two strongly connected components: an undirected star and an undirected cycle. We assume that there are directed edges starting from the cycle and ending at the star (master–slave formalism). We modify the graph by adding directed edges of arbitrarily large weights starting from the star and ending at the cycle (opposite direction of the cutset). We provide criteria (based on the sizes of the star and cycle, the coupling structure, and the weights of cutset and modification edges) that determine how the modification affects the spectral gap of the Laplacian matrix. We apply our approach to understand the modifications that either enhance or hinder synchronization in networks of chaotic Lorenz systems as well as Rössler. Our results show that the hindrance of collective dynamics due to link additions is not atypical as previously anticipated by modification analysis and thus allows for better control of collective properties.

Keywords Laplacian matrix · Spectral gap · Braess’s paradox · Eigenvalue modification · Eigenvalue perturbation · Global perturbation · Network modification · Spectral analysis

Mathematics Subject Classification 05C82 · 34D06 · 82B26 · 93C73 · 05C50 · 90B10 · 47A11 · 47A55

Communicated by Christian Bick.

✉ Sajjad Bakrani
sajjad.bakrani@khas.edu.tr

✉ Narcicegi Kiran
narcicegi.kiran@khas.edu.tr

¹ Faculty of Engineering and Natural Sciences, Kadir Has University, 34083 Istanbul, Turkey

² Instituto de Ciências Matemáticas e Computação, Universidade de São Paulo, São Carlos, Brasil

³ Department of Mathematics, Imperial College London, London SW7 2AZ, UK

Contents

1	Introduction
1.1	Informal Statements of Our Results
1.1.1	Adjacency Matrices and Graph Laplacians
1.1.2	Results (Informal Version)
2	Applications to Synchronization
2.1	Synchronization of Coupled Lorenz Oscillators
2.2	Hindering Synchronization
2.3	Enhancing Synchronization
3	Problem Setting and Results
4	The Laplacian Matrices
4.1	The Laplacian L_G of the Unmodified Graph and Its Spectrum
4.2	The Laplacian L_{G_p} of the Modified Graph
5	Proofs of the Main Results
5.1	Preliminaries, Definitions, and Notations
5.2	Our Approach for Investigating the Spectrum of the Modified Laplacian L_{G_p}
5.2.1	Analysis of P_2
5.2.2	Analysis of P_1
5.3	Proof of Theorem B
5.3.1	Proof of Lemma 14
5.4	Proof of Theorem C
6	Conclusions
A	Synchronization of Coupled Rössler Oscillators
A.1	Hindering Synchronization
A.2	Enhancing Synchronization
B	Technical Lemmas
	References

1 Introduction

Many systems in nature are modeled as networks of interacting units with examples ranging from neuroscience (Ermentrout and Terman 2010) to engineering (Newman 2018). Recent work has revealed that the network interaction structure plays a crucial role in the network emergent dynamics (Eroglu et al. 2017; Prasad et al. 2010; Louodop et al. 2019; Aguiar et al. 2019; Field 2015). Predicting the impact of the network structure on the dynamics is an intricate nonlinear problem that leads to many unexpected results. Indeed, in some situations improving the network structure may lead to functional failures such as Braess's paradox (Eldan et al. 2017) and synchronization loss (Pade and Pereira 2015; Nishikawa and Motter 2010). In large networks depending on the interaction function and isolated dynamics of the nodes, a topological hub may fail to be a functional hub (Pereira et al. 2020; Eguiluz et al. 2005).

The effects of network topology on dynamical phenomena, such as synchronization, diffusion and random walks, can be related to spectral properties of the graph, see, for instance, (Chung 1997; Eroglu et al. 2017). Indeed, to predict the consequences of network modification on the dynamics, one needs to investigate the highly nonlinear changes in the spectrum of the graph Laplacian (Poignard et al. 2019; Pade and Pereira 2015; Biyikoglu et al. 2007).

Although certain correlations between network structure and dynamics have been observed in experimental (Hart et al. 2015) and theoretical (Pade and Pereira 2015;

Milanese et al. 2010) investigations, most of these results are concerned with small modifications to the network. There is a lack of rigorous results to determine the relationship between the network structure and its dynamic properties for arbitrary size modifications. Most of the results in this direction rely on the modification theory of eigenvalues to determine which structural changes are detrimental to the network dynamics. However, previous results relying on perturbation theory suggest that desynchronizing the network by adding new links is unusual (Poignard et al. 2019). To understand this problem, we need to unveil the full nonlinear picture and deal with large changes in the topology.

Networks are a combination of motifs that dictate dynamical behavior and provide resilience to the overall system (Ma'ayan et al. 2008; Kashtan and Alon 2005). We focus on two motifs of complex networks—a cycle and a star—since they are the main constituents of important networks. Indeed, cycles are typical components in the nervous system (Alexander et al. 1986) and orientation tuning in visual cortex (Ben-Yishai et al. 1997). Also, in the context of neuroscience highly connected nodes, called hubs, play a fundamental role in the network (Bonifazi et al. 2009). These networks with hubs are modeled as a collection of star motifs, and each star motif is capable of generating intricate dynamics (Vlasov et al. 2015), as well as their overall interaction (Tönjes et al. 2021).

Although both cycle and star motifs were investigated for noteworthy network dynamics such as collective behavior (Mersing et al. 2021; Muni and Provata 2020; Kantner and Yanchuk 2013; Manik et al. 2017; Corder et al. 2023) and both motifs have a fully developed spectral theory (Brouwer and Haemers 2011) their eigenvectors and eigenvalues can be fully described (as in the case of rings where the matrices are circulant), when these motifs are coupled, the eigenvalues problem becomes an intricate nonlinear problem that remains open.

In this paper, we consider models of networks consisting of cycles and stars coupled in a master–slave topology. Although our problem is dynamics-motivated, we state our main results in a graph theoretic form and consider the synchronization as an application. This is because, in a broader sense, the spectral properties of the graph Laplacian are important in the study of graph connectedness and, hence, any phenomena related to this concept (Mohar 1997).

1.1 Informal Statements of Our Results

We consider three models illustrated in Figs. 1, 2, and 3. All these three models have a master–slave structure, a cycle C_n , a star S_m , and cutset edge(s) starting from the cycle and ending at the hub of the star. We modify these networks and break the master–slave structure by adding directed links from the star to the cycle (red-color edges in the figures).

1.1.1 Adjacency Matrices and Graph Laplacians

Let G be a weighted directed graph (digraph) whose nodes are labeled by $1, \dots, n$. We define the adjacency matrix of G by $A_G = (A_{ij})$, where $A_{ij} \geq 0$ is the weight

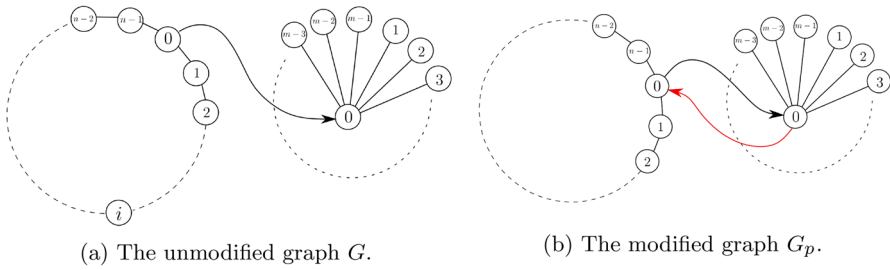


Fig. 1 Model I: breaking the master–slave through hub coupling. We add a directed link from the hub of the star to the cutset node (the red-color edge) where the cutset node refers to the node which the cutset edge starts from and the weakly connected graph becomes strongly connected. The weight of each of the black-color edges is one, while the weight of the red-color edge (modification edge) is arbitrary (Color figure online)

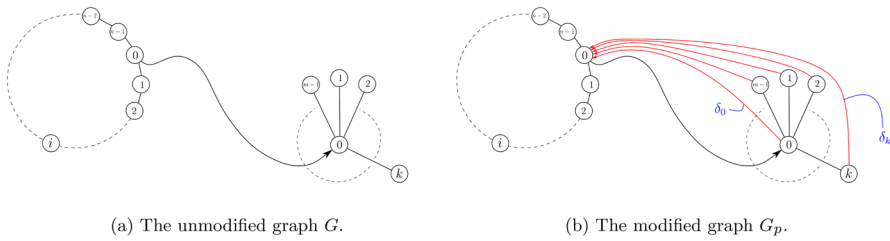


Fig. 2 Model II: breaking the master–slave through multiple couplings. We add links from some nodes of the star to the cutset node of the cycle. The weight of each of the black-color edges is one, while the weights of the red-color edges (modification edges) are arbitrary (Color figure online)

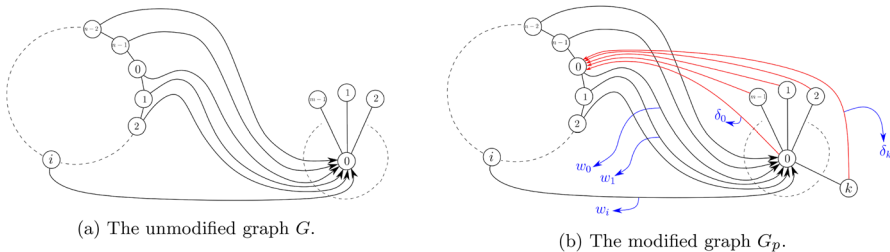


Fig. 3 Model III: breaking the generalized master–slave through multiple couplings. We add links from nodes of the star to the one cutset node of the cycle. The weight of each of the black-color edges is one, while the weights of the red-color edges (modification edges) are arbitrary (Color figure online)

of the directed edge starting from node j and ending at node i . The in-degree of a node is the sum of the weights of the edges that the node receives from other nodes, i.e., the in-degree of the node i is $\sum_j A_{ij}$. We define the Laplacian matrix of G by $L_G := D_G - A_G$, where D_G is a diagonal matrix whose (i, i) -entry is the in-degrees of the node i of G . Let L_G and L_{G_p} represent the Laplacians of the unmodified and modified graphs, respectively. Let $\lambda_2(L_G)$ and $\lambda_2(L_{G_p})$ be the associated second minimum eigenvalues, so-called spectral gap. Our results explain how the modification

affects the spectral gap of the Laplacian matrices of these models. We provide more details in Sect. 4.

1.1.2 Results (Informal Version)

Assume $\delta_0 \geq 0$ is the weight of the modification edge starting from the hub and $\delta \geq 0$ is the sum of the weights of all the modification edges. In model I, we have $\delta_0 = \delta$, and in the other two models, $\delta_0 \leq \delta$. Let m and n be the sizes of the star and cycle, respectively. The term $o(1)$ in the informal statements of Theorems A and B (resp. Theorem C) stands for a function of m (resp. (m, w)) that converges to 0 as $m \rightarrow \infty$ (resp. $\frac{m}{w} \rightarrow \infty$). When the weight of the modification is small, we will call this modification local. This is because the results follow from local analysis of the eigenvalues. If the weight of the modification is large, we called it global, as the analysis requires global techniques to gain insights on the eigenvalues. These models are discussed precisely in Sect. 3. Here, we give an informal version of our main results.

Theorem A (Informal statement) *Consider model I illustrated in Fig. 1. Let the modification $\delta > 0$ be arbitrary. (It does not need to be sufficiently small.) We have*

1. *Although L_{G_p} is not necessarily symmetric, all of its eigenvalues are real.*
2. *There exists a critical cycle size $n_c = \pi\sqrt{m+1}[1+o(1)]$ such that $\lambda_2(L_{G_p}) < \lambda_2(L_G)$ if and only if $n \geq n_c$.*

We illustrate Theorem A in Fig. 4.

To give the informal statement of Theorem B, let $\rho := \frac{\delta_0}{\delta}$. This ratio can be seen as a measure of the modification that the cycle receives from the hub of the star relative to the modification it receives from the leaves of the star. We have $\rho \leq 1$, and by setting $\rho = 1$, the model II reduces to model I.

Theorem B (Informal statement) *Consider model II illustrated in Fig. 2. We have*

1. *Under a local modification, the statement of Theorem A is valid for model II. When $\delta > 0$ is sufficiently small, all the eigenvalues of L_{G_p} are real and the modification decreases the spectral gap if and only if the size of the cycle is larger than the critical value $n_c(m)$.*
2. *Under a global modification (δ be arbitrary), the statement of Theorem A is valid for model II when $\rho > K$, where $0 < K < 1$ is a constant given in Sect. 3.*
3. *Under a global modification (δ be arbitrary), we have $\text{Re}(\lambda_2(L_{G_p})) < \lambda_2(L_G)$ if the size of the cycle is larger than a critical value $n_c^*(m) = 2\pi\sqrt{m+1}[1+o(1)]$.*

Theorem C (Informal statement) *Consider model III illustrated in Fig. 3. Let w be the sum of the weights of all cutset edges. There exist two critical $n_c(m, w)$ and $n_c^*(m, w)$ such that $n_c^* \approx 2n_c = 2\pi\sqrt{\frac{m}{w}+1}[1+o(1)]$, and*

1. *Under a local modification, we have*
 - (a) *if $n > n_c^*(m, w)$, then $\lambda_2(L_{G_p}) \leq \lambda_2(L_G)$.*

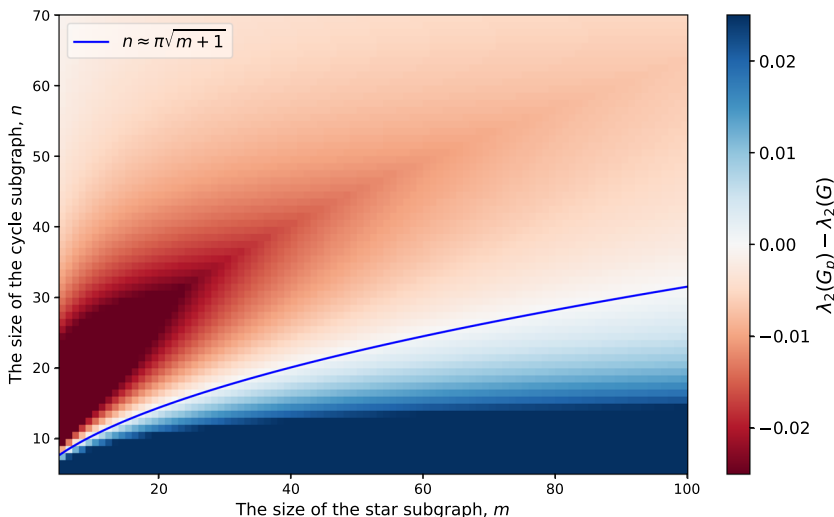


Fig. 4 A comparison of the cases in Theorem A and computations of $\lambda_2(G_p) - \lambda_2(G)$. We create a graph G as described in model 1a with cycle C_n and star S_m subgraphs whose sizes are n and m , respectively. Then, we modify the network as shown in model 1b where $\delta_0 = 1$ and calculate the difference $\lambda_2(G_p) - \lambda_2(G)$ to characterize the behavior of the second minimum eigenvalue after modification. The red color of grids corresponds to a decrease in the second minimum eigenvalue after modification, and the blue color of grids corresponds to an increase in the second minimum eigenvalue after modification, where the intensity of the color at each grid shows the size of the difference $\lambda_2(G_p) - \lambda_2(G)$. Simultaneously, the blue curve given by $n_c = \pi\sqrt{m+1}$ is shown. Thus, regions separated by the blue curve manifest the signature of $\lambda_2(G_p) - \lambda_2(G)$ and it corresponds to the critical transition between the cases stated in Theorem A, i.e., decreasing or increasing behavior of the second minimum eigenvalue after modification (Color figure online)

- (b) if $n_c(m, w) < n < n_c^*(m, w)$, then both increasing and decreasing in the spectral gap can happen. See Theorem C for the distinction between cases.
- (c) if $n < n_c(m, w)$, then $\lambda_2(L_{G_p}) > \lambda_2(L_G)$.

2. Under a global modification, if $n > n_c^*(m, w)$, then $\text{Re}(\lambda_2(L_{G_p})) \leq \lambda_2(L_G)$.

In all three mentioned models, we consider the scenario in which the cutset edges start from the cycle and end at the hub of the star, briefly called the hub connection. Another scenario that can be considered is where the cutset edges end at the leaves of the star instead of its hub, briefly called leaf connection. Our numerical investigation shows that there exists a critical n'_c analogous to n_c in Theorem A and a critical $n'^*_c(m)$ analogous to $n^*_c(m)$ in Theorem B for the leaf connection. However, n'_c is bounded below by n_c ; likewise $n'^*_c(m)$ is bounded below by $n^*_c(m)$. In other words, if we compare the incidence number of $\lambda_2(L_{G_p}) < \lambda_2(L_G)$ for hub and leaf connection, hub connection maximizes the incidence number of $\lambda_2(L_{G_p}) < \lambda_2(L_G)$ for the same parameter set.

The Laplacian matrix L_G of the unmodified graph in all the models I, II, and III is a block lower-triangular matrix, see the form (10). However, adding a modification in the opposite direction of the cutset breaks the triangular structure of L_G , which turns

the analysis of its spectral gap into a non-trivial problem. Our approach to analyzing the changes in the spectral gap consequent to the graph modification is to investigate a secular equation of the Laplacian matrix and its roots. Our analysis is not restricted to the local modification;¹ we indeed analyze the change in the spectral gap under modification of arbitrary size. This requires further work on not only analyzing the modification of spectral gap but also understanding the modifications and distribution of the whole spectrum of the Laplacian matrix.

2 Applications to Synchronization

We consider synchronization in networks of diffusively coupled oscillators as an application. Consider a triplet $\mathcal{G} = (G, f, H)$, where G is a weighted digraph, and $f, H \in C^1(\mathbb{R}^l)$ for $l \geq 1$. The triplet \mathcal{G} defines a system of the form

$$\dot{x}_i = f(x_i) + \Theta \sum_{j=1}^N A_{ij} H(x_j - x_i), \quad i = 1, 2, \dots, N, \quad (1)$$

where $\Theta \geq 0$ is called the coupling strength. Each variable x_i represents the state of the i th node of G , the function f describes the isolated dynamics at each node, and the function H is called the coupling function. We call the triplet \mathcal{G} or its associated system (1) a network of diffusively coupled (identical) systems.

We define the synchronization manifold as

$$M := \{(x_1, \dots, x_N) : x_1 = \dots = x_N \in U\}. \quad (2)$$

We say that a network \mathcal{G} synchronizes if there exists an open neighborhood V of M such that the forward orbit of any point in V converges to M . It is shown (Pereira et al. 2014) that for a network \mathcal{G} with a coupling strength Θ , if

1. the graph G has a spanning diverging tree, and
2. there exists an inflowing open ball $U \subset \mathbb{R}^l$ which is invariant with respect to the flow of the isolated system $\dot{x} = f(x)$, and we have $\|Df(x)\| \leq K$ for some $K > 0$ and all $x \in U$, and
3. we have $H(0) = 0$; moreover, all the eigenvalues of $DH(0)$ are real and positive,

then there exists $\Theta_c \geq 0$ such that when $\Theta \geq \Theta_c$, \mathcal{G} synchronizes. We call

$$\Theta_c = \frac{\rho}{\operatorname{Re}(\lambda_2)}, \quad (3)$$

the critical coupling strength where $\rho = \rho(f, DH(0))$ is a constant. Note that if the third assumption is not fulfilled, the synchronization condition (3) may no longer be

¹ note that even for investigating local changes in the spectral gap, the standard approach, see, e.g., Theorem 6.3.12 in Horn and Johnson (2012), cannot be applied since the spectral gaps in our models are not necessarily simple.

valid. However, in this case, new synchronization conditions may be obtained under the framework of master stability function formalism (Eroglu et al. 2017). Relation (3) with assumptions stated above gives us a criterion to compare synchronizability in networks. More precisely,

Definition 1 Consider two networks $\mathcal{G}_1 = (G_1, f_1, H_1)$ and $\mathcal{G}_2 = (G_2, f_2, H_2)$ that satisfy the assumptions above. Let $\Theta_c(\mathcal{G}_1)$ and $\Theta_c(\mathcal{G}_2)$ be the critical coupling strengths of \mathcal{G}_1 and \mathcal{G}_2 , respectively. We say that \mathcal{G}_1 is more synchronizable than \mathcal{G}_2 if $\Theta_c(\mathcal{G}_1) < \Theta_c(\mathcal{G}_2)$.

Having $\Theta_c(\mathcal{G}_1) < \Theta_c(\mathcal{G}_2)$ means that \mathcal{G}_1 synchronizes for a larger range of Θ than \mathcal{G}_2 . Let us now consider the case that two networks \mathcal{G}_1 and \mathcal{G}_2 only differ in their topology, i.e., having the same isolated dynamics and coupling functions, while the graph structures can be different. In this case, following (3), the spectral gaps of the underlying graphs of the networks determine which one is more synchronizable.

Let consider two networks $\mathcal{G}_1 = (G_1, f, H)$ and $\mathcal{G}_2 = (G_2, f, H)$ that satisfy the assumptions above. Moreover, let $\lambda_2(G_1)$ and $\lambda_2(G_2)$ be the spectral gaps of G_1 and G_2 , respectively. The network \mathcal{G}_1 is more synchronizable than \mathcal{G}_2 if and only if $\lambda_2(G_1) > \lambda_2(G_2)$.

2.1 Synchronization of Coupled Lorenz Oscillators

We consider the following settings for model II given in Fig. 2: Two networks $\mathcal{G} = (G, f, H)$ and $\mathcal{G}_p = (G_p, f, H)$ are generated, where G and G_p are the unmodified and the modified graphs, respectively. The chosen isolated dynamics f is the Lorenz oscillator

$$\begin{aligned}\dot{x} &= \sigma(y - x), \\ \dot{y} &= x(\gamma - z) - y, \\ \dot{z} &= xy - \beta z,\end{aligned}\tag{4}$$

where $\sigma = 10$, $\gamma = 28$, $\beta = 8/3$. Here, H is the identity function on \mathbb{R}^3 . For the described setting, Eq. (3) can be written as $\Theta_c = \frac{\kappa}{\text{Re}(\lambda_2)}$, where κ is defined as in Section 5 of Eroglu et al. (2017). We numerically find that $\kappa \approx 0.9$. So, the expected values of $\Theta_c(\mathcal{G})$ and $\Theta_c(\mathcal{G}_p)$ are calculated accordingly. We examine two experiments to reveal how link addition can lead to synchronization in the network \mathcal{G}_p or break the synchronization in the initial network \mathcal{G} (see Figs. 5 and 6). The network of coupled Lorenz oscillators in model II is simulated to show the synchronization error

$$\langle E \rangle = \sum_{i \neq j} \frac{\|x_i - x_j\|}{(n+m)(n+m-1)}.\tag{5}$$

It is worth mentioning that the same simulations that we have done for the Lorenz system can be done for other systems as well. Indeed, similar results hold as long as the initial conditions lead to an attractor in the synchronization manifold that is contained in a compact set.

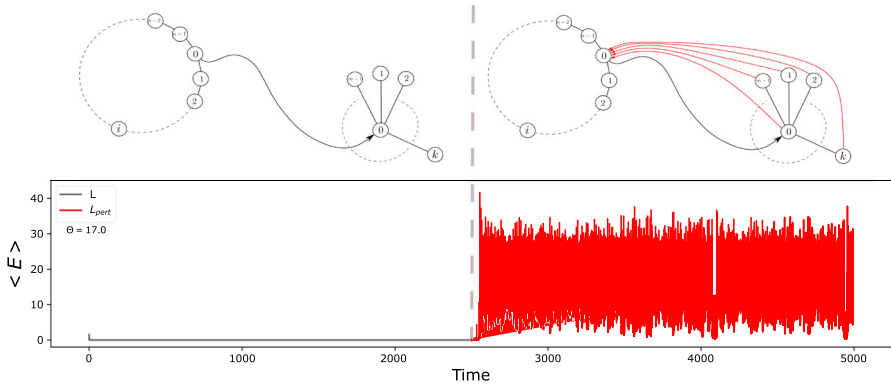


Fig. 5 Hindrance of synchronization due to link addition: Networks of coupled Lorenz oscillators in model II are simulated to show the synchronization error. The sizes of the cycle and star subgraphs are set to $n = 15$ and $m = 15$, and subgraphs are connected via a directed link from the cycle subgraph to the star subgraph where $w_0 = 1$. We consider $H = \mathbf{I}$ as the coupling function. We choose initial conditions randomly selected from the uniform distribution over $[3.5, 5)$ and integrate the network until time $t = 2500$ s. The system goes into synchronization after some transient. At $t = 2500$ s, we add the red links to the system, i.e., $\delta_i = 1$, where $i = 0, 1, \dots, m - 1$, and perturb the system by adding noise randomly selected from the uniform distribution over $[0.01, 0.02)$ to each state, then the synchronization loss occurs and the system does not return into synchronization after transient time. Note that $\alpha_1 = 0.04$, $\beta_{15,1}^- = 0.06$ in Theorem B

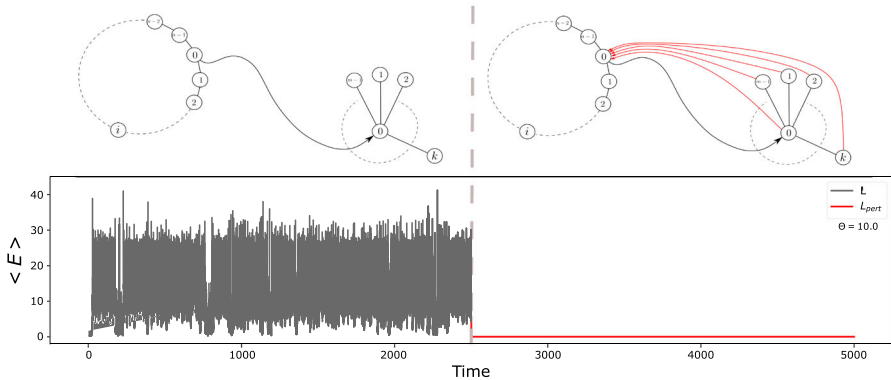


Fig. 6 Enhancement of synchronization due to link addition: networks of coupled Lorenz oscillators in model II are simulated to show the synchronization error. The sizes of the cycle and star subgraphs are set to $n = 9$ and $m = 15$, and subgraphs are connected via a directed link from the cycle subgraph to the star subgraph where $w_0 = 1$. We consider $H = \mathbf{I}$ as the coupling function. We choose initial conditions randomly selected from the uniform distribution over $[3.5, 5)$ and integrate the network until time $t = 2500$ s. After the red links are added to the system at $t = 2500$ s, i.e., $\delta_i = 1$, where $i = 0, 1, \dots, m - 1$, the synchronization occurs where the mean error $\langle E \rangle$ goes to zero. Note that $\alpha_1 = 0.12$, $\beta_{15,1}^- = 0.06$ in Theorem B

2.2 Hinderance Synchronization

To examine the hindrance of synchronization due to link addition, the overall coupling constant Θ is selected such that $\Theta_c(\mathcal{G}) < \Theta < \Theta_c(\mathcal{G}_p)$ (see Fig. 5). Note that such Θ values only exist when $\lambda_2(G) > \lambda_2(G_p)$ due to the order relations of synchronizability stated above. When the selected Θ is above the $\Theta_c(\mathcal{G})$, the trajectories synchronize for the network \mathcal{G} . Then, the system is modified by adding links at a given time t . Since the selected Θ is below the $\Theta_c(\mathcal{G}_p)$, the system loses its synchronization thereafter.

In model II, the sizes of the cycle and star subgraphs are set to $n = 15$ and $m = 15$. The weights of the cutset and modification edges are $w_0 = 1$ and $\delta_i = 1$, where $i = 0, 1, \dots, m - 1$. All initial states are randomly selected from the uniform distribution over $[3.5, 5)$.

2.3 Enhancing Synchronization

To examine the enhancement of synchronization due to link addition, the overall coupling constant Θ is selected such that $\Theta_c(\mathcal{G}_p) < \Theta < \Theta_c(\mathcal{G})$ (see Fig. 6). Note that such Θ values only exist when $\lambda_2(G_p) > \lambda_2(G)$. When the selected Θ is below the $\Theta_c(\mathcal{G})$, the trajectories cannot synchronize for the network \mathcal{G} . Then, the system is modified by adding links at a given time t . Since the selected Θ is above the $\Theta_c(\mathcal{G}_p)$, the system synchronizes.

In model II, the sizes of the cycle and star subgraphs are set to $n = 9$ and $m = 15$. The weights of the cutset and modification edges are $w_0 = 1$ and $\delta_i = 1$, where $i = 0, 1, \dots, m - 1$. All initial states are randomly selected from the uniform distribution over $[3.5, 5)$. Therefore, hindrance and enhancement of synchronization due to link addition manifest themselves in simulations, and it perfectly agrees with the findings of our theorems.

3 Problem Setting and Results

Let G be a weighted directed graph (digraph) whose nodes are labeled by $1, \dots, n$. We assume that G is unilaterally connected. (A digraph is unilaterally connected if for any two arbitrary nodes i and j , there exists a directed path from i to j or j to i .) This implies that the zero eigenvalue of L_G is simple (Veerman and Lyons 2020). It is also an easy consequence of Gershgorin theorem that the real parts of all the non-zero eigenvalues of L_G are positive. Let $\lambda_1, \dots, \lambda_n$ be the eigenvalues of L_G , ordered according to their real parts, i.e.,

$$0 = \lambda_1 < \operatorname{Re}(\lambda_2) \leq \operatorname{Re}(\lambda_3) \leq \dots \leq \operatorname{Re}(\lambda_n).$$

The second minimum (with respect to the real-part ordering) eigenvalue, i.e., λ_2 , is called the spectral gap of G . In this paper, we are interested in how modifying G can affect its spectral gap for models I, II, and III.

Let us start with model I (see Fig. 1a). We define

Definition 2 Consider arbitrary integers $n \geq 3$ and $m \geq 4$, and an arbitrary real number $w \geq 0$. Then,

- for any integer $0 \leq l \leq n$, we define

$$\alpha_l := 2 \left(1 - \cos \frac{l\pi}{n} \right). \tag{6}$$

- we define $\beta_{m,w}^-$ and $\beta_{m,w}^+$ as the roots of the quadratic polynomial $\lambda^2 - (m + w)\lambda + w$, i.e.,

$$\beta_{m,w}^\pm = \frac{1}{2} \left[m + w \pm \sqrt{(m + w)^2 - 4w} \right]. \tag{7}$$

Remark 1 By virtue of Taylor’s theorem, we can approximate α_l for sufficiently small $\frac{l}{n}$ by $\alpha_l \approx \frac{l^2\pi^2}{n^2}$. Regarding $\beta_{m,w}^\pm$, when $(m + w)^2 \gg 4w$, we can approximate $\beta_{m,w}^+$ by $m + w$, and $\beta_{m,w}^-$ by

$$\beta_{m,w}^- = \frac{\beta_{m,w}^- \beta_{m,w}^+}{\beta_{m,w}^+} \approx \frac{w}{m + w}. \tag{8}$$

Before we proceed to our first result, let us give some intuition about this definition. The parameter w in $\beta_{m,w}^\pm$ stands for the sum of the weights of all the cutset edges starting from the cycle and ending at the star. In the case of model I and II, we assume $w = 1$, but for model III, we deal with arbitrary w . As it is shown later (see Proposition 1), the spectrum of the unmodified Laplacian L_G is $\{\alpha_l : \text{where } 0 \leq l \leq n \text{ and } l \text{ is even}\} \cup \{\beta_{m,w}^-, 1, \beta_{m,w}^+\}$. Thus, the spectral gap of L_G is given by $\min\{\alpha_2, \beta_{m,w}^-\}$. Although the α_l s for odd l do not appear as the eigenvalues of L_G , they play an important role in our theory. In particular, α_1 appears in the formulation of all the three main results of this paper.

Here is our main result on model I:

Theorem A (Model I) Assume $\beta_{m,1}^- \notin \{\alpha_l : 0 \leq l \leq n\}$. Consider an arbitrary modification $\delta_0 > 0$ and the corresponding Laplacian $L_{G_p} = L_G(\delta_0)$. Then, all the eigenvalues of L_{G_p} are real. Moreover, we have

- (i) if $\alpha_1 < \beta_{m,1}^-$, then $\lambda_2(L_{G_p}) < \lambda_2(L_G)$.
- (ii) if $\beta_{m,1}^- < \alpha_1$, then $\lambda_2(L_{G_p}) > \lambda_2(L_G)$.

Remark 2 The assumption $\beta_{m,1}^- \notin \{\alpha_l : 0 \leq l < n\}$ in this theorem (and also in the next theorem) typically holds for arbitrary m and n .

Let us now discuss model II (see Fig. 2a). Let $\delta_i \geq 0$ be the weight of the edge starting from node i (see Fig. 2b). Thus, model II is reduced to model I by setting $\delta_i = 0$ for $i = 1, \dots, m - 1$. In this strand, we define

Definition 3 Let $\delta_i \geq 0, i = 0, \dots, m - 1$, be the weight of the modification edge starting from node i of the star and ending at node 0 of the cycle. We define $\bar{\delta} := (\delta_0, \dots, \delta_{m-1})$, and $\delta := \delta_0 + \delta_1 + \dots + \delta_{m-1}$.

Obviously, $\bar{\delta} = 0$ if and only if $\delta = 0$. Note also that $\delta = 0$ corresponds to the unmodified graph G . We now state our next main result:

Theorem B (Model II) *Assume $\beta_{m,1}^- \notin \{\alpha_l : 0 \leq l < n\}$. Consider a modification $\bar{\delta} \neq 0$ and let $L_{G_p} = L_G(\bar{\delta})$ be the corresponding Laplacian. Then, the following hold.*

(i) (Local modification) *Let $\bar{\delta} \neq 0$ be a sufficiently small modification. Then, all the eigenvalues of L_{G_p} are real, and*

(a) *If $\alpha_1 < \beta_{m,1}^-$, then $\lambda_2(L_{G_p}) < \lambda_2(L_G)$.*

(b) *If $\beta_{m,1}^- < \alpha_1$, then $\lambda_2(L_{G_p}) > \lambda_2(L_G)$.*

(ii) (Global modification) *Let $\bar{\delta} \neq 0$ be an arbitrary modification. We have*

(a) *If $\alpha_2 < \beta_{m,1}^-$, then $\text{Re}(\lambda_2(L_{G_p})) < \lambda_2(L_G)$.*

(b) *Assume the condition $\delta < \delta_0\beta_{m,1}^+$ is satisfied. Then, all the eigenvalues of L_{G_p} are real, and the statements (iia) and (iib) of this theorem also hold for the modification $\bar{\delta}$.*

This theorem is proved in Sect. 5.3. Let us mention a few remarks.

Remark 3 Note that, by setting $\delta = \delta_0$, Theorem A directly follows from Theorem B.

Remark 4 In spite of Theorem A for which the main statements hold for a modification of arbitrary size, in Theorem B, we require a condition on the modification, i.e., $\delta < \delta_0\beta_{m,1}^+$, to make the statements for modifications of arbitrary size. Roughly speaking, this is due to the possibility of the emergence of non-real eigenvalues. Indeed, as it is shown in the proof of Theorem B, for small modification $\bar{\delta} \neq 0$, the modified Laplacian L_{G_p} has two real eigenvalues in the interval (α_{n-1}, ∞) . However, as $\bar{\delta}$ varies and gets larger in size, these two real eigenvalues may collide and become a pair of complex conjugates. In this case, we can think of the scenario in which the real part of these eigenvalues decreases such that for some sufficiently large modification $\bar{\delta}$, these eigenvalues become the spectral gap of L_{G_p} . By assuming $\delta < \delta_0\beta_{m,1}^+$, we indeed avoid this scenario.

We now discuss model III (see Fig. 3a). Let $w_i \geq 0$, where $i = 0, \dots, n-1$, be the weight of the edge starting from node i of the cycle. Without loss of generality, assume $w_0 > 0$. We also define

Definition 4 Let w_i be as mentioned above. We define $\bar{w} = (w_0, \dots, w_{n-1})$ and $w = w_0 + w_1 + \dots + w_{n-1}$.

We show later that $\lambda_2(L_G) = \min\{\alpha_2, \beta_{m,w}^-\}$. Regarding the modification in the case of model III, we consider the same family of modifications as we considered in model II: For every $0 \leq i \leq m-1$, there exists a modification edge with weight $\delta_i \geq 0$ starting from node i of the star and ending at node 0 of the cycle (see Fig. 3b). Let $\bar{\delta}$ and δ be as in Definition 3. For given m, n, \bar{w}, δ_0 and δ , in the case that $\alpha_2 \neq \beta_{m,w}^-$, we also define

$$S = S(m, n, \bar{w}, \delta_0, \delta) := \delta - \frac{\delta - \delta_0\alpha_2}{\alpha_2^2 - (m+w)\alpha_2 + w} \sum_{i=0}^{n-1} w_i \cos \frac{2i\pi}{n}. \quad (9)$$

As it is shown later, the sign of S determines if the characteristic polynomial of L_{G_p} , i.e., $\det(L_{G_p} - \lambda I)$, decreases or increases at the point $\lambda = \alpha_2$. Our last main result is as follows.

Theorem C (Model III) *Assume $\beta_{m,w}^- \notin \{\alpha_l : 0 \leq l \leq n\}$. Consider a modification $\bar{\delta} \neq 0$ and let $L_{G_p} = L_G(\bar{\delta})$ be the corresponding Laplacian. Then, the following hold.*

(i) *(Local modification) Let $\bar{\delta} \neq 0$ be sufficiently small. Then, all the eigenvalues of L_{G_p} are real, and we have*

(a) *If $\alpha_2 < \beta_{m,w}^-$ and $S < 0$, then $\lambda_2(L_{G_p}) < \lambda_2(L_G)$.*

(b) *If $\alpha_2 < \beta_{m,w}^-$ and $S > 0$, then $\lambda_2(L_{G_p}) = \lambda_2(L_G)$.*

(c) *If $0 < \beta_{m,w}^- < \alpha_1$, then $\lambda_2(L_{G_p}) > \lambda_2(L_G)$.*

(d) *If $\alpha_1 < \beta_{m,w}^- < \alpha_2$ and $\sum_{i=0}^{n-1} w_i \cos(\frac{n}{2} - i)\theta > 0$, where $\theta = \pi - \cos^{-1}(\frac{\beta_{m,w}^- - 2}{2})$, then $\lambda_2(L_{G_p}) > \lambda_2(L_G)$.*

(e) *If $\alpha_1 < \beta_{m,w}^- < \alpha_2$ and $\sum_{i=0}^{n-1} w_i \cos(\frac{n}{2} - i)\theta < 0$, where $\theta = \pi - \cos^{-1}(\frac{\beta_{m,w}^- - 2}{2})$, then $\lambda_2(L_{G_p}) < \lambda_2(L_G)$.*

(ii) *(Global modification) Let $\bar{\delta} \neq 0$ be an arbitrary modification and assume $\alpha_2 < \beta_{m,w}^-$.*

(a) *If $S < 0$, then $\text{Re}(\lambda_2(L_{G_p})) < \lambda_2(L_G)$.*

(b) *If $S > 0$, then $\text{Re}(\lambda_2(L_{G_p})) \leq \lambda_2(L_G)$.*

4 The Laplacian Matrices

4.1 The Laplacian L_G of the Unmodified Graph and Its Spectrum

In this section, we investigate the spectrum of the unmodified Laplacian matrix L_G . Denote the Laplacian matrices of the cycle C_n and the star S_m by L_{C_n} and L_{S_m} , respectively. Then,

$$L_G := \begin{pmatrix} L_{C_n} & 0 \\ -C & L_{S_m} + D_C \end{pmatrix}, \tag{10}$$

where

$$L_{C_n} = \begin{pmatrix} 2 & -1 & & -1 \\ -1 & 2 & \ddots & \\ & \ddots & \ddots & -1 \\ -1 & & -1 & 2 \end{pmatrix} \quad \text{and} \quad L_{S_m} = \begin{pmatrix} m-1 & -\mathbf{1}_{m-1}^\top \\ -\mathbf{1}_{m-1} & I_{m-1} \end{pmatrix}.$$

Moreover, for models I and II, we have

$$C = \begin{pmatrix} 1 & 0_{1 \times (n-1)} \\ 0_{(m-1) \times 1} & 0_{(m-1) \times (n-1)} \end{pmatrix} \quad \text{and} \quad D_C = \begin{pmatrix} 1 & 0_{1 \times (m-1)} \\ 0_{(m-1) \times 1} & 0_{(m-1) \times (m-1)} \end{pmatrix}, \quad (11)$$

and for model III, we have

$$C = \begin{pmatrix} w_0 & w_1 & \cdots & w_{n-1} \\ & 0_{(m-1) \times n} & & \end{pmatrix} \quad \text{and} \quad D_C = \begin{pmatrix} w & 0_{1 \times (m-1)} \\ 0_{(m-1) \times 1} & 0_{(m-1) \times (m-1)} \end{pmatrix}. \quad (12)$$

The block triangular form of L_G implies $\sigma(L_G) = \sigma(L_{C_n}) \cup \sigma(L_{S_m} + D_C)$. Thus, to study $\sigma(L_G)$, we need to investigate each of $\sigma(L_{C_n})$ and $\sigma(L_{S_m} + D_C)$ individually. In this strand, we have the following lemmas.

Lemma 1 *Recall Definition 2. We have $\sigma(L_{C_n}) = \{\alpha_l : \text{where } 0 \leq l \leq n \text{ and } l \text{ is even}\}$. Moreover, the multiplicity of all the eigenvalues except for 0 and 4 (the eigenvalue 4 appears only when n is even) is 2.*

Proof See Brouwer and Haemers (2011).

Lemma 2 *Let C and D_C be as in (12). Then, $\sigma(L_{S_m} + D_C) = \{\beta_{m,w}^-, 1, \beta_{m,w}^+\}$, where $\beta_{m,w}^\pm$ are as in (7). Moreover, the eigenvalues $\beta_{m,w}^-$ and $\beta_{m,w}^+$ are simple, and the eigenvalue 1 is of multiplicity $m - 2$.*

Proof This lemma is a special case of Lemma B.2, which is proved in Appendix B.

The previous two lemmas give the spectrum of the unmodified Laplacian L_G :

Proposition 1 *We have $\sigma(L_G) = \{\alpha_l : \text{where } 0 \leq l \leq n \text{ and } l \text{ is even}\} \cup \{\beta_{m,w}^-, 1, \beta_{m,w}^+\}$.*

Remark 5 We assume that $m \geq 4$, i.e., the star S_m has at least four nodes. It is straightforward to show that for any $m \geq 4$ and $w > 0$, we have $\beta_{m,w}^- < 1$ and $4 < \beta_{m,w}^+$. On the other hand, $0 \leq \alpha_l = 2(1 - \cos \frac{l\pi}{n}) \leq 4$, for all $0 \leq l \leq n$. This means that $\beta_{m,w}^+$ is a simple eigenvalue of L_G .

4.2 The Laplacian L_{G_p} of the Modified Graph

Consider model III and observe that the modified Laplacian matrix L_{G_p} is given by

$$L_{G_p} := \begin{pmatrix} L_{C_n} + D_\Delta & -\Delta \\ -C & L_{S_m} + D_C \end{pmatrix}, \quad (13)$$

where C and D_C are as in (12),

$$\Delta = \begin{pmatrix} \delta_0 & \delta_1 & \cdots & \delta_{m-1} \\ & 0_{(n-1) \times m} & & \end{pmatrix} \quad \text{and} \quad D_\Delta = \begin{pmatrix} \delta & 0_{1 \times (n-1)} \\ 0_{(n-1) \times 1} & 0_{(n-1) \times (n-1)} \end{pmatrix}. \quad (14)$$

Notation 1 For the sake of convenience, we set $L_1 := L_{C_n} + D_\Delta$ and $L_2 := L_{S_m} + D_C$.

Using this notation, Laplacian (13) is written as

$$L_{G_p} = \begin{pmatrix} L_1 & -\Delta \\ -C & L_2 \end{pmatrix}. \quad (15)$$

The Laplacian L_{G_p} of the modified graph of model II is of the form (15), where C and D_C are as in (11), and Δ and D_Δ are given by (14).

The Laplacian L_{G_p} of the unmodified graph of model I is also of the form (15), where C and D_C are as in (11), and Δ and D_Δ are given by

$$\Delta = \begin{pmatrix} \delta_0 & 0_{1 \times (m-1)} \\ 0_{(n-1) \times 1} & 0_{(n-1) \times (m-1)} \end{pmatrix} \quad \text{and} \quad D_\Delta = \begin{pmatrix} \delta & 0_{1 \times (n-1)} \\ 0_{(n-1) \times 1} & 0_{(n-1) \times (n-1)} \end{pmatrix}. \quad (16)$$

Here (model I), we have $\delta_0 = \delta$.

Notice that, in all these three models, despite the unmodified Laplacian L_G , the modified Laplacian L_{G_p} does not have a triangular form. Due to this reason, analysis of the spectrum of L_{G_p} requires further work. We deal with this analysis in the next section.

5 Proofs of the Main Results

In this section, we prove our main results: Theorems B and C (Theorem A follow from Theorem B). Note that model II can be considered as a special case of model III. Thus, it is reasonable to introduce the main concepts and notations of the proofs in this section mainly based on model III. This section is organized as follows. We first discuss some preliminaries, definitions, and notations in Sect. 5.1. In Sect. 5.2, we discuss the techniques that are used in the proofs of the theorems. We then prove Theorem B in Sect. 5.3. Finally, we prove Theorem C in Sect. 5.4.

5.1 Preliminaries, Definitions, and Notations

In this section, we discuss some preliminaries and introduce some concepts and notations which are used throughout the proofs.

Notation 2 Throughout, $\mathbf{1}_k$ stands for the k -dimensional vector whose entries are all 1. We may drop k when it is clear from the context.

Definition 5 Let w , δ_0 and δ be real, and m and k be positive integers. Consider $\lambda \in \mathbb{R}$.

(i) We define $\mu : \lambda \mapsto \mu(\lambda)$ by

$$\mu = \mu(\lambda) = \frac{1 - \lambda}{\lambda^2 - (m + w)\lambda + w}, \quad (17)$$

and $y : \lambda \mapsto y(\lambda)$ by

$$y = y(\lambda) = \frac{\delta - \delta_0 \lambda}{\lambda^2 - (m + w) \lambda + w}. \quad (18)$$

(ii) For any $k \geq 3$, we define

$$Q_k = Q_k(\lambda) = \begin{pmatrix} \lambda - 2 & 1 & & & \\ 1 & \lambda - 2 & 1 & & 0 \\ & & 1 & \ddots & \ddots \\ 0 & & & \ddots & \ddots & 1 \\ & & & & 1 & \lambda - 2 \end{pmatrix}_{k \times k}. \quad (19)$$

The next two lemmas investigate the matrix $Q_k(\lambda)$ for different values of $\lambda > 0$. See Hu and O'Connell (1996) for the proofs.²

Lemma 3 Assume $0 < \lambda < 4$ and let $\theta = \pi - \cos^{-1}(\frac{\lambda-2}{2})$. We have

- (i) $\det(Q_k) = \frac{(-1)^k \sin(k+1)\theta}{\sin \theta}$.
 (ii) the matrix $R = Q_k^{-1}$ exists for $\theta \neq \frac{l\pi}{k+1}$ ($l = 1, \dots, k$) and is given by

$$R_{ij} = \frac{\cos(k+1 - |i-j|)\theta - \cos(k+1 - i - j)\theta}{2 \sin \theta \sin(k+1)\theta}, \quad \text{for } 1 \leq i, j \leq k. \quad (20)$$

Lemma 4 Assume $\lambda \geq 4$ and let $\theta = \cosh^{-1}(\frac{\lambda-2}{2})$. Then,

- (i) for $\lambda > 4$, we have $\det(Q_k) = \frac{\sinh(k+1)\theta}{\sinh \theta}$.
 (ii) for $\lambda = 4$, we have $\det(Q_k) = k + 1$.
 (iii) The inverse matrix $R = Q_k^{-1}$ exists for all $\lambda \geq 4$ and is given by

$$R_{ij} = (-1)^{i+j} \cdot \frac{\cosh(k+1 - |i-j|)\theta - \cosh(k+1 - i - j)\theta}{2 \sinh \theta \sinh(k+1)\theta}, \quad \text{for } 1 \leq i, j \leq k. \quad (21)$$

Recall α_l defined by (6). By Lemmas 3 and 4, and a straightforward calculation, we have

Lemma 5 The matrix $Q_{n-1}(\lambda)$ is invertible if and only if $\lambda \neq \alpha_l$ for $l = 1, \dots, n-1$.

5.2 Our Approach for Investigating the Spectrum of the Modified Laplacian L_{G_p}

In this section, we discuss the method we use to investigate the spectrum of the modified Laplacian L_{G_p} . We directly apply this method to study model III and then use the results to investigate models I and II.

² Regarding Lemma 3, the formulas in Hu and O'Connell (1996) are not totally correct. In this current paper, we have used the corrected ones. Note also that θ in this current paper is not the same as in Hu and O'Connell (1996).

Recall that the modified Laplacian of model III is given by

$$L_{G_p} = \begin{pmatrix} L_1 & -\Delta \\ -C & L_2 \end{pmatrix}, \tag{22}$$

where L_1 and L_2 are as in Notation 1, and the matrices C and Δ are given by (12) and (14), respectively. Our study of the eigenvalues of L_{G_p} is based on the following lemma.

Lemma 6 Consider the modified Laplacian L_{G_p} given by (22). For $\lambda \in \mathbb{R}$, we have

- (i) if $\lambda \notin \sigma(L_1)$, then $\det(L_{G_p} - \lambda I) = \det(L_1 - \lambda I) \cdot P_1(\lambda)$, where $P_1(\lambda) = \det(M_1)$, for $M_1 = M_1(\lambda) = L_2 - \lambda I - C(L_1 - \lambda I)^{-1}\Delta$.
- (ii) if $\lambda \notin \sigma(L_2)$, then $\det(L_{G_p} - \lambda I) = \det(L_2 - \lambda I) \cdot P_2(\lambda)$, where $P_2(\lambda) = \det(M_2)$, for $M_2 = M_2(\lambda) = L_1 - \lambda I - \Delta(L_2 - \lambda I)^{-1}C$.
- (iii) for $i = 1, 2$, we have that $\lambda_0 \notin \sigma(L_i)$ is an eigenvalue of L_{G_p} with algebraic multiplicity k , if and only if $P_i(\lambda_0) = P'_i(\lambda_0) = \dots = \frac{d^{k-1}P_i}{d\lambda^{k-1}}(\lambda_0) = 0$, and $\frac{d^k P_i}{d\lambda^k}(\lambda_0) \neq 0$.

Remark 6 Lemma 6 allows us to count the multiplicity of $\lambda_0 \in \sigma(L_{G_p})$ when $\lambda_0 \notin \sigma(L_1) \cap \sigma(L_2)$. However, this lemma may give information about the multiplicity of λ_0 when $\lambda_0 \in \sigma(L_1) \cap \sigma(L_2)$ as well. This is important for us since we have such eigenvalues in our models. Let λ_0 be such an eigenvalue. Since $\lambda_0 \in \sigma(L_1)$, the matrix $(L_1 - \lambda_0 I)^{-1}$ does not exist. However, depending on the matrices C and Δ , the expression $\lim_{\lambda \rightarrow \lambda_0} Y(\lambda)$, where $Y(\lambda) := C(L_1 - \lambda_0 I)^{-1}\Delta$, may exist. This allows us to define M_1 and P_1 at $\lambda = \lambda_0$ by taking the limit $\lambda \rightarrow \lambda_0$. Now, if $Y(\lambda)$ at $\lambda = \lambda_0$ is smooth enough, then the multiplicity of λ_0 as an eigenvalue of L_{G_p} is $l + k$, where l is the multiplicity of λ_0 as an eigenvalue of L_1 and k is the integer that satisfies $P_1(\lambda_0) = P'_1(\lambda_0) = \dots = \frac{d^{k-1}P_1}{d\lambda^{k-1}}(\lambda_0) = 0$, and $\frac{d^k P_1}{d\lambda^k}(\lambda_0) \neq 0$. Analogous holds when $\lambda_0 \in \sigma(L_2)$ but $\Delta(L_2 - \lambda I)^{-1}C$ is well defined and smooth enough at $\lambda = \lambda_0$.

According to Lemma 6, an eigenvalue λ of L_{G_p} that is not in $\sigma(L_1) \cap \sigma(L_2)$ must satisfy $P_1(\lambda) = 0$ or $P_2(\lambda) = 0$. The proofs of our results are based on the analysis of these two equations. Sections 5.2.1 and 5.2.2 are dedicated to this analysis.

Before we proceed further, let us show that $\lambda = 1$ is an eigenvalue of L_{G_p} for any arbitrary $\bar{\delta}$.

Lemma 7 For arbitrary $\bar{\delta}$, we have $1 \in \sigma(L_{G_p})$. Moreover, the (algebraic and geometric) multiplicity of 1 is at least $m - 2$.

Proof Recall that $L_{G_p} = \begin{pmatrix} L_1 & -\Delta \\ -C & L_2 \end{pmatrix}$. It follows from the proof of Lemma B.2 (see relation (B5)) that there exist $m - 2$ linearly independent left eigenvectors v such that $v^\top L_2 = v^\top$. Moreover, any such a vector v is of the form $v = (0, v_1, \dots, v_{m-1}) \in \mathbb{R}^m$. (The first entry is zero.) Consider the vector $u := (0, v) \in \mathbb{R}^{n+m}$. Taking into

account that, except for the first row, all the entries of C are zero (see (12)), we obtain

$$u^\top L_{G_p} = (0_{1 \times n}, v^\top) \begin{pmatrix} L_1 & -\Delta \\ -C & L_2 \end{pmatrix} = (0_{1 \times n}, v^\top L_2) = u^\top.$$

This means that for such vs , the corresponding vectors u are left eigenvectors of L_{G_p} associated with the eigenvalue 1. This proves the lemma.

5.2.1 Analysis of P_2

In this section, we investigate the matrix $M_2(\lambda)$ and the function $P_2(\lambda) := \det(M_2(\lambda))$ introduced in Lemma 6 for model III. We first need to analyze the matrix $L_2 - \lambda I$ and its inverse:

Lemma 8 Recall μ from (17). We have

- (i) the function μ is well defined at $\lambda \notin \{\beta_{m,w}^-, \beta_{m,w}^+\}$.
(ii) for $\lambda \in \mathbb{R} \setminus \sigma(L_2) = \{\beta_{m,w}^-, 1, \beta_{m,w}^+\}$, we have

$$(L_2 - \lambda I)^{-1} = \begin{pmatrix} m-1+w-\lambda & -\mathbf{1}^\top \\ -\mathbf{1} & (1-\lambda)I \end{pmatrix}^{-1} = \begin{pmatrix} \mu & \frac{\mu}{1-\lambda} \mathbf{1}^\top \\ \frac{\mu}{1-\lambda} \mathbf{1} & \frac{1}{1-\lambda} I + \frac{\mu}{(1-\lambda)^2} \mathbf{1} \mathbf{1}^\top \end{pmatrix}. \quad (23)$$

Proof Item (i) is straightforward. Item (ii) follows from Lemma B.17.

We now start to calculate $M_2 = M_2(\lambda) = L_1 - \lambda I - \Delta(L_2 - \lambda I)^{-1}C$. The expression $(L_2 - \lambda I)^{-1}$ is well defined at $\lambda \notin \sigma(L_2) = \{\beta_{m,w}^-, 1, \beta_{m,w}^+\}$. By a straightforward calculation and using relation (23), for $\lambda \notin \sigma(L_2)$, we have $\Delta(L_2 - \lambda I)^{-1}C = yC$, where $y = y(\lambda)$ is given by (18). Note that y , and therefore yC , is well defined and smooth at $\lambda = 1$. In other words, although $(L_2 - \lambda I)^{-1}$ is not defined at $\lambda = 1$ (because $1 \in \sigma(L_2)$), the expression $\Delta(L_2 - \lambda I)^{-1}C$ can be defined at $\lambda = 1$, and so do the matrix M_2 and the function P_2 . This was discussed earlier in Remark 6. We give the following lemma to emphasize this property.

Lemma 9 The function $P_2(\lambda) = \det(M_2)$ is well defined and smooth at $\lambda \notin \{\beta_{m,w}^-, \beta_{m,w}^+\}$.

Having $\Delta(L_2 - \lambda I)^{-1}C = yC$, we obtain

$$M_2 = M_2(\lambda) = \left(\begin{array}{c|c} \begin{matrix} 2-\lambda+\delta-w_0y & -1-w_1y-w_2y \cdots w_{n-2}y-1-w_{n-1}y \\ -1 \\ 0_{(n-3) \times 1} \\ -1 \end{matrix} & -Q_{n-1} \end{array} \right), \quad (24)$$

where $Q_{n-1} = Q_{n-1}(\lambda)$ is the symmetric tridiagonal matrix given by (19). Applying Lemma B.17 on this matrix, for $\lambda \notin \{\beta_{m,w}^-, \beta_{m,w}^+\}$ such that $Q_{n-1}(\lambda)$ is invertible

(recall that, by Lemma 5, the matrix $Q_{n-1}(\lambda)$ is invertible if and only if $\lambda \neq \alpha_l$ for $l = 1, \dots, n - 1$), we obtain

$$P_2(\lambda) = \det(M_2) = (-1)^{n-1} \det(Q_{n-1}) [\xi(\delta, \lambda) - y\psi(w, \lambda)], \tag{25}$$

where

$$\xi(\delta, \lambda) = 2 - \lambda + \delta + R_{11} + R_{1n-1} + R_{n-1,1} + R_{n-1,n-1}, \tag{26}$$

for which $R = (R_{ij})_{1 \leq i, j \leq n-1}$ is the inverse of Q_{n-1} , and

$$\psi = \psi(\bar{w}, \lambda) = w_0 - \sum_{i=1}^{n-1} w_i [R_{i1} + R_{in-1}]. \tag{27}$$

Lemmas 3 and 4 give some formulas for $R = Q_{n-1}^{-1}$. Substituting these formulas in (26) and (27) gives

Lemma 10 *For the functions $\xi(\delta, \lambda)$ and $\psi(\bar{w}, \lambda)$, we have*

$$\xi = \xi(\delta, \lambda) = \begin{cases} \delta - 2 \sin \theta \tan \frac{n\theta}{2}, & 0 < \lambda < 4 \text{ and } \theta = \pi - \cos^{-1}(\frac{\lambda-2}{2}), \\ \delta + \frac{2}{\lambda} \cdot [(-1)^n - 1], & \lambda = 4, \\ \delta + \frac{2 \sinh \theta}{\sinh n\theta} \cdot [(-1)^n - \cosh n\theta], & \lambda > 4 \text{ and } \theta = \cosh^{-1}(\frac{\lambda-2}{2}), \end{cases}$$

and

$$\psi = \psi(\bar{w}, \lambda) = \begin{cases} \frac{1}{\cos \frac{n\theta}{2}} \sum_{i=0}^{n-1} w_i \cos(\frac{n}{2} - i)\theta, & 0 < \lambda < 4 \text{ and } \theta = \pi - \cos^{-1}(\frac{\lambda-2}{2}), \\ \sum_{i=0}^{n-1} (-1)^i w_i, & n \text{ is even, } \lambda = 4, \\ \sum_{i=0}^{n-1} (-1)^i w_i [1 - \frac{2i}{n}], & n \text{ is odd, } \lambda = 4, \\ \frac{1}{\cosh \frac{n\theta}{2}} \sum_{i=0}^{n-1} (-1)^i w_i \cosh(\frac{n}{2} - i)\theta, & n \text{ is even, } \lambda > 4 \text{ and } \theta = \cosh^{-1}(\frac{\lambda-2}{2}), \\ \frac{1}{\sinh \frac{n\theta}{2}} \sum_{i=0}^{n-1} (-1)^i w_i \sinh(\frac{n}{2} - i)\theta, & n \text{ is odd, } \lambda > 4 \text{ and } \theta = \cosh^{-1}(\frac{\lambda-2}{2}). \end{cases}$$

Proof For $\lambda \neq 4$, the proof is a straightforward calculation by substituting (20) and (21) into (26) and (27). For the case of $\lambda = 4$, the proof follows from taking the limit of the formulas for the cases $\lambda \neq 4$ as $\lambda \rightarrow 4$ and using L'Hôpital's rule.

This lemma together with relation (25), gives some formulas for $P_2(\lambda)$ when P_2 is well defined ($\lambda \notin \{\beta_{m,w}^-, \beta_{m,w}^+\}$) and $Q_{n-1}(\lambda)$ is invertible, i.e., $\lambda \neq \alpha_l$ for $l = 1, \dots, n - 1$. However, we can use (25) to calculate P_2 at $\lambda = \alpha_l$ by taking $\lim P_2(\lambda)$ as $\lambda \rightarrow \alpha_l$. By this trick, we have that (25) is well defined and smooth at every real $\lambda \notin \{\beta_{m,w}^-, \beta_{m,w}^+\}$.

To make the analysis of P_2 simpler, we consider two different cases of $0 \leq \lambda < 4$ and $\lambda \geq 4$. For the first case, let $\theta = \pi - \cos^{-1}(\frac{\lambda-2}{2})$, and define $p(\theta) := P_2(\lambda(\theta)) = P_2(2[1 - \cos \theta])$. For $0 < \theta < \pi$ such that $2[1 - \cos \theta] \notin \{\beta_{m,w}^-, \beta_{m,w}^+\}$, this gives

$$p(\theta) = 2[\cos n\theta - 1] + \delta \cdot \frac{\sin n\theta}{\sin \theta} - 2y \cdot \frac{\sin \frac{n\theta}{2}}{\sin \theta} \sum_{i=0}^{n-1} w_i \cos\left(\frac{n}{2} - i\right)\theta. \tag{28}$$

Observe that $p(0) = \lim_{\theta \rightarrow 0^+} p(\theta) = 0$. With a straightforward calculation, we can also obtain:

Lemma 11 Recall α_l given by (6) and assume $\alpha_l = 2(1 - \cos \frac{l\pi}{n}) \notin \{\beta_{m,w}^-, \beta_{m,w}^+\}$, where $l \in \mathbb{Z}$ is as specified below. Then,

- (i) for even $0 \leq l \leq n-1$, we have $p(\frac{l\pi}{n}) = 0$.
- (ii) for odd $1 \leq l \leq n-1$, we have $p(\frac{l\pi}{n}) = -4 - \frac{2y}{\sin \frac{l\pi}{n}} \sum_{i=0}^{n-1} w_i \sin \frac{il\pi}{n}$.
- (iii) for even $1 \leq l \leq n-1$, we have

$$p' \left(\frac{l\pi}{n} \right) = \frac{n}{\sin \frac{l\pi}{n}} \left[\delta - y \sum_{i=0}^{n-1} w_i \cos \frac{il\pi}{n} \right]. \quad (29)$$

5.2.2 Analysis of P_1

In this section, we investigate the matrix M_1 and the function $P_1(\lambda) = \det(M_1(\lambda))$ introduced in Lemma 6 for model III. We start with analyzing the matrix $L_1 - \lambda I$ and its inverse. Note that

$$L_1 - \lambda I = \left(\begin{array}{c|c} 2 + \delta - \lambda & -1 \quad 0_{1 \times (n-3)} \quad -1 \\ \hline -1 & \\ 0_{(n-3) \times 1} & -Q_{n-1} \\ -1 & \end{array} \right). \quad (30)$$

Lemma 12 Let $\lambda > 0$ be real. Then, the matrix $L_1 - \lambda I$ is invertible if and only if $\lambda \neq \alpha_l$ and $\xi(\delta, \lambda) \neq 0$, where $1 < l \leq n-1$ is even and $\xi(\delta, \lambda)$ is given by (26).

Proof Assume Q_{n-1} is invertible. Applying Lemma B.17 on matrix (30) gives

$$\det(L_1 - \lambda I) = (-1)^{n-1} \det(Q_{n-1}) \xi(\delta, \lambda).$$

This proves the lemma for the case that Q_{n-1} is invertible.

Now, we consider the case that Q_{n-1} is singular. It follows from Lemma 5 that $Q_{n-1}(\lambda)$ is invertible if and only if $\lambda \neq \alpha_l$ for $l = 1, \dots, n-1$. Equivalently Q_{n-1} is singular if and only if $0 < \lambda = 2[1 - \cos \theta_0] < 4$ and $\sin n\theta_0 = 0$ (see also Lemmas 3 and 4). By virtue of Lemma 10, for $\lambda = 2[1 - \cos \theta_0]$, we obtain

$$\begin{aligned} \det(L_1 - \lambda I) &= \lim_{\theta \rightarrow \theta_0} \det(L_1 - \lambda I) = \lim_{\theta \rightarrow \theta_0} \frac{\sin n\theta}{\sin \theta} \cdot \left(\delta - 2 \sin \theta \tan \frac{n\theta}{2} \right) \\ &= 2(\cos n\theta_0 - 1). \end{aligned}$$

Thus, when Q_{n-1} is singular, $L_1 - \lambda I$ is invertible if and only if $\cos n\theta_0 \neq 1$, i.e., $\lambda \neq \alpha_l$ where $2 \leq l \leq n-1$ is even. This ends the proof.

For real $\lambda > 0$, assume $\xi(\delta, \lambda) \neq 0$ and consider the case that $R = Q_{n-1}^{-1}$ exists. Then, $L_1 - \lambda I$ is invertible, and by Lemma B.17, we have

$$(L_1 - \lambda I)^{-1} = \begin{pmatrix} \xi^{-1} & -\xi^{-1}r^\top \\ -\xi^{-1}r & -R + \xi^{-1}rr^\top \end{pmatrix},$$

where $r = (R_{11} + R_{1n-1}, R_{21} + R_{2n-1}, \dots, R_{n-11} + R_{n-1n-1})^\top$. This gives

$$M_1 = M_1(\lambda) = \left(\begin{array}{c|c} m-1+w-\lambda-\frac{\delta_0\psi}{\xi} & -1-\frac{\delta_1\psi}{\xi} \quad -1-\frac{\delta_2\psi}{\xi} \quad \dots \quad -1-\frac{\delta_{m-1}\psi}{\xi} \\ \hline -\mathbf{1}_{m-1} & (1-\lambda)I \end{array} \right),$$

where $\psi = \psi(w, \lambda)$ is given by (27). Then, by virtue of Lemma B.2, we have

Lemma 13 For real $\lambda > 0$, assume $R = Q_{n-1}^{-1}$ exists, and $\xi(\delta, \lambda) \neq 0$. Then, $\lambda \neq 1$ is an eigenvalue of L_{G_p} if and only if

$$\lambda^2 - \left[m + w - \frac{\delta_0\psi}{\xi} \right] \lambda + w - \frac{\delta\psi}{\xi} = 0, \tag{31}$$

or equivalently, one of the following holds:

$$\lambda = \frac{1}{2} \left(m + w - \sqrt{(m+w)^2 - 4w + \frac{4(\delta - \delta_0\lambda)\psi}{\xi}} \right) \tag{32}$$

or

$$\lambda = \frac{1}{2} \left(m + w + \sqrt{(m+w)^2 - 4w + \frac{4(\delta - \delta_0\lambda)\psi}{\xi}} \right).$$

Remark 7 If $\lambda \notin \{\beta_{m,w}^-, \beta_{m,w}^+\}$, then relation (31) can be derived from the equation $\xi - y\psi = 0$ (see (25)), and vice versa. In other words, if $\lambda \neq \beta_{m,w}^\pm$, then relation (31) does not give any further information about the eigenvalue λ other than what $P_2 = 0$ gives, where P_2 is given by (25). However, since P_2 is not defined at $\beta_{m,w}^\pm$ (because μ is not defined at these points), we still require (31) to analyze $\lambda = \beta_{m,w}^\pm$.

5.3 Proof of Theorem B

In this section, we prove Theorem B. Throughout this section, we assume that $w_0 = 1$ and $w_i = 0$, where $1 \leq i \leq n-1$. Moreover, we have that $\delta \geq \delta_0 \geq 0$. Note that, to adapt this proof for the case of Theorem A, it is sufficient to assume $\delta = \delta_0$. We start with the following definition.

Definition 6 Recall Definition 2. Assume $\beta_{m,1}^- \notin \{\alpha_l : 0 \leq l \leq n\}$ and let $\kappa \geq 2$ be the even integer such that $\beta_{m,1}^- \in (\alpha_{\kappa-2}, \alpha_\kappa)$.

- (i) Define $J_{\beta^-} := (\alpha_{\kappa-2}, \alpha_\kappa)$.

(ii) Let $2 \leq l \leq n - 2$ be even. We define

$$J_l = \begin{cases} (\alpha_{l-1}, \alpha_l), & \text{if } 2 \leq l < \kappa, \\ (\alpha_l, \alpha_{l+1}), & \text{if } \kappa \leq l \leq n - 2. \end{cases}$$

(iii) Define $J_{\beta^+} := (\alpha_{n-1}, \infty)$.

(iv) For the sake of convenience, we define the set of indices $\mathcal{I} := \{\beta^-, \beta^+\} \cup \{l : 0 < l < n \text{ and } l \text{ is even}\}$.

Remark 8 Note that when $\kappa = 2$, there does not exist J_l for $2 \leq l < \kappa$.

Remark 9 Notice that $\beta_{m,1}^+ > m \geq 4$, and so $\beta_{m,1}^+ \in J_{\beta^+}$.

Considering eigenvalues with their multiplicities, the modified Laplacian L_{G_p} has $n + m$ eigenvalues. The next lemma describes where these $n + m$ eigenvalues are located.

Lemma 14 Let $\bar{\delta} \neq 0$ be an arbitrary modification that satisfies $\delta < \delta_0 \beta_{m,1}^+$. Then, all the $n + m$ eigenvalues of the modified Laplacian L_{G_p} of model II are real and given by the union of the following four disjoint groups (see also Remark 11).

- (i) L_{G_p} has $\lfloor \frac{n-1}{2} \rfloor + 1$ real eigenvalues given by $\{\alpha_l : \text{where } 0 \leq l \leq n - 1 \text{ and } l \text{ is even}\}$.
- (ii) L_{G_p} has $m - 2$ of repeated eigenvalue $\lambda = 1$.
- (iii) Recall the set \mathcal{I} . Each interval J_γ for $\gamma \in \mathcal{I}$ and $\gamma \neq \beta^+$ contains exactly one real eigenvalue of L_{G_p} (except possibly for the $m - 2$ eigenvalues 1 counted in item (ii)). We have $\lfloor \frac{n}{2} \rfloor$ of these intervals, and so L_{G_p} has $\lfloor \frac{n}{2} \rfloor$ real eigenvalues given by these intervals.
- (iv) The interval J_{β^+} contains two real eigenvalues of the modified Laplacian L_{G_p} . Thus, L_{G_p} has 2 eigenvalues given by J_{β^+} .

Remark 10 Observe that $(\lfloor \frac{n-1}{2} \rfloor + 1) + (m - 2) + \lfloor \frac{n}{2} \rfloor + 2 = n + m$.

Remark 11 The sets of the eigenvalues given by items (i) and (ii) might not be disjoint, i.e., $\alpha_l = 1$ for some even l . The same may happen for (ii) and (iii), i.e., the eigenvalue in J_γ given by item (iii) equals to 1. The eigenvalue 1 in such scenarios are counted separately from the $m - 2$ eigenvalues 1 given in item (ii). In such scenarios, the multiplicity of eigenvalue 1 is $m - 1$.

The proof of Lemma 14 is postponed to Sect. 5.3.1. We now prove Theorem B.

Part (i) of Theorem B follows from Theorem C which is proved later in Sect. 5.4. Here, we show that part (i) of Theorem B satisfies the corresponding assumptions of Theorem C. Recall S given by (9). Setting $w_0 = 1$ and $w_i = 0$, where $1 \leq i \leq n - 1$, gives

$$S = \frac{\alpha_2 [\delta (\alpha_2 - m) + \delta_0 - \delta]}{(\alpha_2 - \beta_{m,1}^-) (\alpha_2 - \beta_{m,1}^+)} \quad (33)$$

and

$$\sum_{i=0}^{n-1} w_i \cos\left(\frac{n}{2} - i\right)\theta = \cos\frac{n\theta}{2}, \quad \text{where} \quad \theta = \pi - \cos^{-1}\left(\frac{\beta_{m,1}^- - 2}{2}\right). \quad (34)$$

Take into account that $\delta_0 \leq \delta$ and $\alpha_2 < 4$. When $\alpha_2 < \beta_{m,1}^-$, we have $S < 0$. On the other hand, when $\alpha_1 < \beta_{m,1}^- < \alpha_2$, we have $\frac{\pi}{n} < \theta < \frac{2\pi}{n}$ and so $\cos\frac{n\theta}{2} < 0$, where θ is as above. Therefore, part (iia) of Theorem B follows from parts (iia) and (iie) of Theorem C, and part (iib) of Theorem B follows directly from part (iic) of Theorem C.

Part (iia) of Theorem B is a consequence of part (iia) of Theorem C, since, as mentioned above, when $\alpha_2 < \beta_{m,1}^-$, we have $S < 0$.

Let us now prove part (iib) of Theorem B. First, assume $\alpha_2 < \beta_{m,1}^-$. This implies $\kappa > 2$. Thus, by Lemma 14, L_{G_p} has a unique eigenvalue in the interval $J_2 = (\alpha_1, \alpha_2)$ which is indeed the spectral gap of L_{G_p} . Denote it by $\lambda_2(L_{G_p})$. Since the spectral gap of the unmodified Laplacian L_G is α_2 , we have $\lambda_2(L_{G_p}) < \lambda_2(L_G)$. This shows that, in the case $\alpha_2 < \beta_{m,1}^-$, the statement of part (iia) of Theorem B holds for arbitrary modification $\bar{\delta}$ that satisfies $\delta < \delta_0\beta_{m,1}^+$.

Now, assume $\beta_{m,1}^- < \alpha_2$. This implies $\kappa = 2$, i.e., $J_{\beta^-} = (0, \alpha_2)$. According to Lemma 14, L_{G_p} has a unique eigenvalue in the interval $J_{\beta^-} = (0, \alpha_2)$ which is indeed the spectral gap of L_{G_p} . Denote it by $\lambda_2(\bar{\delta})$. Note that the spectral gap of the unmodified graph L_G is $\lambda_2(0) = \beta_{m,1}^-$. Following Lemma 13, we have

$$\lambda_2(\bar{\delta}) = \frac{1}{2} \left(m + 1 - \sqrt{(m + 1)^2 - 4 + \frac{4[\delta - \delta_0\lambda_2(\bar{\delta})]}{\xi}} \right), \quad (35)$$

where $\xi = \xi(\delta, \lambda_2(\bar{\delta})) = \delta - 2\sin\theta \tan\frac{n\theta}{2}$ and $\theta = \pi - \cos^{-1}(\frac{\lambda_2(\bar{\delta}) - 2}{2})$. Observe that when $\bar{\delta} = 0$ (and consequently, $\delta = \delta_0 = 0$), $\lambda_2(0) = \beta_{m,1}^-$ satisfies this relation. According to (35), the proof follows from this observation that for a given $\bar{\delta}$, we have $\lambda_2(\bar{\delta}) > \lambda_2(0)$, $\lambda_2(\bar{\delta}) = \lambda_2(0)$ and $\lambda_2(\bar{\delta}) < \lambda_2(0)$ if and only if the expression

$$\frac{\delta - \delta_0\lambda_2(\bar{\delta})}{\xi} \quad (36)$$

be negative, zero, and positive, respectively.

First, consider the case $\alpha_1 < \lambda_2(0) = \beta_{m,1}^- < \alpha_2$. It is easily seen that $\beta_{m,1}^- \leq \beta_{4,1}^- \approx 0.21$ for all $m \geq 4$. Thus, having $\alpha_1 = 2(1 - \cos\frac{\pi}{n}) < \beta_{m,1}^- < 0.21$ yields $n \geq 7$ which implies $\alpha_2 = 2(1 - \cos\frac{2\pi}{n}) < 1$. Note also that as $\bar{\delta}$ changes, $\lambda_2(\bar{\delta})$ remains in $(0, \alpha_2)$. (This is a consequence of part (iii) of Lemma 14.) Therefore,

$$\delta - \delta_0\lambda_2(\bar{\delta}) > \delta - \delta_0 + \delta_0[1 - \alpha_2] \geq \max\{\delta - \delta_0, \delta_0[1 - \alpha_2]\}. \quad (37)$$

Thus, the numerator of (36) is positive for any $\bar{\delta} \neq 0$. Regarding the denominator of (36), note that $\xi(0, \beta_{m,1}^-) > 0$ when $\alpha_1 < \beta_{m,1}^- < \alpha_2$. We claim that $\xi(\delta, \lambda_2(\bar{\delta})) > 0$ for all $\bar{\delta}$. Taking into account that ξ is a smooth function of (δ, λ) for $\lambda \neq \alpha_1$, the claim will be proved once we show that $\lambda_2(\bar{\delta}) > \alpha_1$ holds for any $\bar{\delta}$ and also ξ does not vanish as $\bar{\delta}$ varies.

We first show that $\lambda_2(\bar{\delta}) > \alpha_1$ for all $\bar{\delta}$. Assume the contrary; there exists $\bar{\delta}^\dagger$ and correspondingly δ^\dagger and δ_0^\dagger for which $\lambda_2(\bar{\delta}^\dagger) = \alpha_1$. However, $\lim_{\delta \rightarrow \delta^\dagger} \xi = \infty$. On the other hand, the numerator of (36) converges to $\delta^\dagger - \delta_0^\dagger \alpha_1 > 0$. Therefore, as $\delta \rightarrow \delta^\dagger$, expression (36) converges to zero which, by (35), implies that $\lambda_2(\bar{\delta}^\dagger) = \beta_{m,1}^-$ and so $\beta_{m,1}^- = \alpha_1$. This contradicts the assumption $\beta_{m,1}^- \notin \{\alpha_l : 0 \leq l < n\}$ of Theorem B. Thus, $\lambda_2(\bar{\delta}) < \alpha_1$ for all $\bar{\delta}$.

Since $\alpha_1 < \lambda_2(\bar{\delta}) < \alpha_2$ for all $\bar{\delta}$, we have that $\sin \theta \tan \frac{n\theta}{2} < 0$, where $\theta = \pi - \cos^{-1}(\frac{\lambda_2(\bar{\delta}) - \alpha_1}{\alpha_2 - \alpha_1})$. This yields $\xi > \delta$ for all $\bar{\delta}$ which means that it cannot vanish as $\bar{\delta}$ varies. Therefore, the numerator and denominator of (36) are positive. It then follows from (37) that when $\alpha_1 < \beta_{m,1}^- < \alpha_2$, we have $\lambda_2(L_{G_p}) < \lambda_2(L_G)$, as desired.

Now, we consider the case $0 < \lambda_2(0) = \beta_{m,1}^- < \alpha_1$. We first show that $\lambda_2(\bar{\delta}) < \alpha_1$ for all $\bar{\delta}$. Assume the contrary; there exists $\bar{\delta}^\dagger$ and correspondingly δ^\dagger and δ_0^\dagger for which $\lambda_2(\bar{\delta}^\dagger) = \alpha_1$. However, $\lim_{\delta \rightarrow \delta^\dagger} \xi = -\infty$. On the other hand, the numerator of (36) converges to $\delta^\dagger - \delta_0^\dagger \alpha_1 \geq 0$ (note that $\alpha_1 \leq 1$ for all $n \geq 3$). Therefore, as $\delta \rightarrow \delta^\dagger$, expression (36) converges to zero which, by (35), implies that $\lambda_2(\bar{\delta}^\dagger) = \beta_{m,1}^-$ and so $\beta_{m,1}^- = \alpha_1$. This contradicts the assumption $\beta_{m,1}^- \notin \{\alpha_l : 0 \leq l < n\}$ of Theorem B. Thus, $\lambda_2(\bar{\delta}) < \alpha_1$ for all $\bar{\delta}$.

It is easily seen that $\xi(0, \beta_{m,1}^-) < 0$ when $0 < \beta_{m,1}^- < \alpha_1$. We claim that $\xi(0, \beta_{m,1}^-) < 0$ for all $\bar{\delta}$. Note that ξ is a smooth function for $\lambda \neq \alpha_1$. On the other hand, we have shown that $\lambda_2(\bar{\delta}) < \alpha_1$ for all $\bar{\delta}$. Thus, to prove the claim, we need to show that ξ does not vanish as $\bar{\delta}$ varies. Assume the contrary; there exists $\bar{\delta}^\dagger$ and correspondingly δ^\dagger and δ_0^\dagger such that as $\bar{\delta} \rightarrow \bar{\delta}^\dagger$, we have $\xi(\delta, \lambda_2(\bar{\delta}^\dagger)) \rightarrow 0$. By (35), this requires the numerator of (36) to vanish at $\bar{\delta}^\dagger$, i.e., $\delta^\dagger - \delta_0^\dagger \lambda_2(\bar{\delta}^\dagger) = 0$. However, by $\lambda_2(\bar{\delta}) < \alpha_1$ and taking into account that $\alpha_1 \leq 1$ for all $n \geq 3$, we obtain

$$\delta^\dagger - \delta_0^\dagger \lambda_2(\bar{\delta}^\dagger) \geq \max \left\{ \delta^\dagger - \delta_0^\dagger, \delta_0^\dagger \left[1 - \lambda_2(\bar{\delta}^\dagger) \right] \right\} > 0. \quad (38)$$

This contradicts the assumption of vanishing ξ at $\bar{\delta}^\dagger$. Therefore, we have $\xi(0, \beta_{m,1}^-) < 0$ for all $\bar{\delta}$. It then follows from (37) that when $0 < \beta_{m,1}^- < \alpha_1$, we have $\lambda_2(L_{G_p}) > \lambda_2(L_G)$, as desired. This finishes the proof of part (iib) and the proof of Theorem B.

5.3.1 Proof of Lemma 14

So far, we have used Lemma 14 to prove Theorem B. We are now in the position of proving this lemma.

The proof of Lemma 14 is based on Lemma 11. In the setting of Theorems A and B, we assume $w_0 = 1$ and $w_i = 0$ for $i = 1, \dots, n - 1$. In this case, (28) is written as

$$p(\theta) = 2[\cos n\theta - 1] + [\delta - y] \cdot \frac{\sin n\theta}{\sin \theta}. \tag{39}$$

Then, Lemma 11 gives

Lemma 15 For $0 \leq \lambda < 4$, let $\theta = \pi - \cos^{-1}(\frac{\lambda-2}{2})$. Consider p given by (39). Then,

- (i) for even $0 \leq l \leq n - 1$, we have $p(\frac{l\pi}{n}) = 0$.
- (ii) for odd $1 \leq l \leq n - 1$, we have $p(\frac{l\pi}{n}) = -4$.
- (iii) for even $1 \leq l \leq n - 1$, we have

$$p' \left(\frac{l\pi}{n} \right) = \frac{n}{\sin \frac{l\pi}{n}} [\delta - y] = \frac{-n\lambda}{\sin \frac{l\pi}{n}} \cdot \frac{(m - \lambda)\delta + \delta - \delta_0}{\lambda^2 - (m + 1)\lambda + 1}. \tag{40}$$

Proof of part (i) of Lemma 14 The proof directly follows from part (i) of Lemma 15.

Proof of part (ii) of Lemma 14 The proof directly follows from Lemma 7 and its proof.

Proof of part (iii) of Lemma 14 We first investigate $p'(\frac{l\pi}{n})$ given by (40). The expression $\lambda^2 - (m + 1)\lambda + 1$ is positive if and only if $\lambda < \beta_{m,1}^-$ or $\lambda > \beta_{m,1}^+ > 4$. For $\lambda = 2[1 - \cos \frac{l\pi}{n}]$, when l is even, this gives

$$\begin{cases} \lambda^2 - (m + 1)\lambda + 1 > 0, & \text{if } l \text{ is even and } 2 \leq l < \kappa, \\ \lambda^2 - (m + 1)\lambda + 1 < 0, & \text{if } l \text{ is even and } \kappa \leq l < n - 1. \end{cases}$$

When $\lambda \in J_\gamma$, for $\gamma \neq \beta^+$, we have that $\lambda < 4 \leq m$. On the other hand, $\delta_0 \leq \delta$. This implies that when $\delta > 0$, we have $(m - \lambda)\delta + \delta - \delta_0 > 0$. Taking into account that $\sin \frac{l\pi}{n} > 0$ for all $0 \leq l \leq n - 1$, we obtain

$$\begin{cases} p' \left(\frac{l\pi}{n} \right) < 0, & \text{if } l \text{ is even and } 2 \leq l < \kappa, \\ p' \left(\frac{l\pi}{n} \right) > 0, & \text{if } l \text{ is even and } \kappa \leq l < n - 1. \end{cases}$$

We have that $p'(\frac{l\pi}{n}) = 0$ if and only if $\delta = 0$. This, together with item (i) of Lemma 15, gives

Proposition 2 Any point of $\{\alpha_l : \text{where } 0 \leq l \leq n - 1 \text{ and } l \text{ is even}\}$ is a multiple eigenvalue of L_G with multiplicity 2, and a simple eigenvalue of L_{G_p} .

For even l , when $2 \leq l < \kappa$, we have $p'(\frac{l\pi}{n}) < 0$. This means that $p(\theta)$ is positive for θ close to $\frac{l\pi}{n}$ and $\theta < \frac{l\pi}{n}$. On the other hand, $p(\frac{(l-1)\pi}{n}) = -4 < 0$. Thus, by the intermediate value theorem, the function p has a root in the interval $(\frac{(l-1)\pi}{n}, \frac{l\pi}{n})$. This implies that L_{G_p} has a real eigenvalue in J_l . Analogously, for even l and when

$\kappa \leq l < n - 1$, the function p has a root in the interval $\left(\frac{l\pi}{n}, \frac{(l+1)\pi}{n}\right)$ which means that L_{G_p} has a real eigenvalue in J_l .

At $\bar{\delta} = 0$ (when there is no modification), the interval J_{β^-} has the eigenvalue $\beta_{m,1}^-$. As $\bar{\delta}$ changes, the eigenvalue $\beta_{m,1}^-$ starts to move. However, since $\alpha_{\kappa-2}$ and α_κ are simple roots, this eigenvalue cannot leave the interval $J_{\beta^-} = (\alpha_{\kappa-2}, \alpha_\kappa)$. This means that L_{G_p} has a real root in J_{β^-} .

We have shown that each interval J_γ for $\gamma \in \mathcal{I}$ and $\gamma \neq \beta^+$ contains at least one real eigenvalue of L_{G_p} . To finish the proof, we need to show that each of these intervals has exactly one eigenvalue (apart from $m - 2$ eigenvalues 1 counted in item (ii) that might be located in one of these intervals). Note that we have already counted $n + m - 2 = \lfloor \frac{n-1}{2} \rfloor + 1 + m - 2 + \lfloor \frac{n}{2} \rfloor$ real eigenvalues of L_{G_p} . The matrix L_{G_p} has $n + m$ eigenvalues. Thus, the proof of part (iii) of this lemma is done after we prove part (iv) of this lemma below. \square

Proof of part (iv) of Lemma 14 So far, we have shown that the matrix L_{G_p} has at least $n + m - 2$ eigenvalues located outside of the interval J_{β^+} , and as $\bar{\delta}$ varies, none of these eigenvalues enters this interval. Notice that for arbitrary $\delta > 0$, when n is even, $p(\frac{(n-1)\pi}{n}) < 0$, and when n is odd, $p(\frac{(n-1)\pi}{n}) = 0$ and $p'(\frac{(n-1)\pi}{n}) \neq 0$. This means that if there is any real eigenvalue located in J_{β^+} , then it cannot leave this interval as $\bar{\delta}$ changes. As shown below, for sufficiently small $\bar{\delta} \neq 0$, the interval J_{β^+} has exactly two real eigenvalues. On the other hand, L_{G_p} is a real matrix. Therefore, if it possesses non-real eigenvalues, then they need to appear as pairs (complex conjugates). This means that, for a given $\bar{\delta}$, we either have two real eigenvalues in J_{β^+} or none. Therefore, the proof of part (iv) of Lemma 14 is done if we show that, under the condition $\delta < \delta_0\beta_{m,1}^+$, the interval J_{β^+} has at least one real eigenvalue.

First, we show that when $\bar{\delta} \neq 0$ is sufficiently small, the interval J_{β^+} has exactly two real eigenvalues. For even n , this is obvious since at $\delta = 0$, we have two eigenvalues $\lambda = 4$ and $\lambda = \beta_{m,1}^+$, and so, as $\bar{\delta}$ varies and remains sufficiently small, these two eigenvalues might move but they remain in J_{β^+} and do not collide (so, they remain real). The case of odd n is similar; since for $\bar{\delta} \neq 0$, we have $p'(\alpha_{n-1}) > 0$ and $p(4) < 0$, the intermediate value theorem implies that there is a root in the interval $(\alpha_{n-1}, 4)$. On the other hand, the eigenvalue $\beta_{m,1}^+ \in (4, \infty)$ of L_G might move as $\bar{\delta}$ varies but as far as $\bar{\delta}$ is sufficiently small, it does not collide with the eigenvalue that we just found in the interval $(\alpha_{n-1}, 4)$. Therefore, we have that for small $\bar{\delta} \neq 0$, the interval J_{β^+} contains exactly two real eigenvalues of L_{G_p} .

We now prove that J_{β^+} has at least one real root when $\delta < \delta_0\beta_{m,1}^+$. Evaluating (25) at $\lambda > 4$ gives

$$P_2(\lambda) = (-1)^{n-1} \cdot \frac{\sinh n\theta}{\sinh \theta} \left[\frac{2 \sinh \theta}{\sinh n\theta} \cdot [(-1)^n - \cosh n\theta] + \delta - \frac{\delta - \delta_0\lambda}{\lambda^2 - (m+1)\lambda + 1} \right],$$

where $\theta = \cosh^{-1}(\frac{\lambda-2}{2})$. Note that $\lambda^2 - (m+1)\lambda + 1$ vanishes at $\lambda = \beta_{m,1}^\pm$. Thus, when $\delta < \delta_0\beta_{m,1}^+$, we have

$$\lim P_2(\lambda) = \begin{cases} +\infty, & \text{for even } n, \text{ as } \lambda \rightarrow (\beta_{m,1}^+)^-, \\ -\infty, & \text{for odd } n, \text{ as } \lambda \rightarrow (\beta_{m,1}^+)^-. \end{cases} \tag{41}$$

When n is even, we have $P_2(4) = \frac{4n[(m-3)\delta - \delta_0]}{13-4m} < 0$. Taking (41) and the fact that P_2 is smooth on $(\alpha_{n-1}, \beta_{m,1}^+)$ into account (see Lemma 9), the intermediate value theorem implies the existence of a real root of P_2 in $(4, \beta_{m,1}^+) \subset J_{\beta^+}$, as desired.

For the case of odd n , we have $p(\frac{(n-1)\pi}{n}) = 0$ and $p'(\frac{(n-1)\pi}{n}) > 0$. Thus, for $\lambda > \alpha_{n-1}$ and close to α_{n-1} , we have $P_2(\lambda) > 0$. Taking (41) and the fact that P_2 is smooth on $(\alpha_{n-1}, \beta_{m,1}^+)$ into account (see Lemma 9), the intermediate value theorem implies the existence of a real root of P_2 in $(\alpha_{n-1}, \beta_{m,1}^+) \subset J_{\beta^+}$, as desired. This ends the proof.

5.4 Proof of Theorem C

We first prove that for sufficiently small $\bar{\delta}$, all the eigenvalues of L_{G_p} are real. It is known that the roots of a polynomial (in our case, the characteristic polynomial of L_{G_p}) depend continuously on the coefficients of that polynomial. Therefore, if $\{\lambda_i(\bar{\delta}) : i = 1, \dots, n + m\}$ is the spectrum of L_{G_p} , then $\lambda_i(\bar{\delta})$ is a continuous function of $\bar{\delta}$. It is a direct consequence of the implicit function theorem that if $\lambda_i(0)$ is a simple eigenvalue of L_G , then for sufficiently small $\bar{\delta}$, we have that $\lambda_i(\bar{\delta})$ is real. Thus, to prove our statement, we need to investigate how multiple eigenvalues of the unmodified Laplacian L_G behave as $\bar{\delta}$ varies.

Recall Proposition 1. According to Remark 5 and the assumption $\beta_{m,w}^- \notin \{\alpha_l : 0 \leq l < n\}$ of the theorem, we have that $\beta_{m,w}^-$ and $\beta_{m,w}^+$ are simple eigenvalues of L_G . Note that $1 \in \{\alpha_l : 0 \leq l \leq n, \text{ and } l \text{ is even}\}$ if and only if $\frac{n}{6}$ is an integer. First, assume $\frac{n}{6} \notin \mathbb{Z}$. In this case, the multiplicity of all the eigenvalues α_l except for 0 and 4 (the eigenvalue 4 appears only when n is even) is 2. However, it follows from Lemma 11 that, for each even l , as $\bar{\delta}$ varies, one of the two eigenvalues α_l remains as an eigenvalue of L_{G_p} for small arbitrary $\bar{\delta}$, and the other eigenvalue moves continuously. This means that from each of the multiple eigenvalues α_l , two real eigenvalues get born. On the other hand, following Lemma 7 and its proof, the eigenvalue 1 remains an eigenvalue of L_{G_p} with multiplicity $m - 2$. This implies that when $\frac{n}{6} \notin \mathbb{Z}$ and $\bar{\delta}$ is sufficiently small, all the eigenvalues of L_{G_p} are real. The case of $\frac{n}{6} \in \mathbb{Z}$ is similar. With the same conclusion, except for $l = \frac{n}{6}$, i.e., $\alpha_l = 1$, two real eigenvalues get born from each eigenvalue α_l , where $l = 1, \dots, n - 1$. Regarding $\alpha_l = 1$ (note that the multiplicity of 1 as an eigenvalue of L_G in this case is m), we have that $\alpha_l = 1$ remains an eigenvalue of L_{G_p} with multiplicity $m - 1$ and a new real eigenvalue gets born from it. This proves that when $\bar{\delta}$ is sufficiently small, all the eigenvalues of L_{G_p} are real.

The rest of the proof of part (i) of Theorem C is based on the following lemma

Lemma 16 Consider p and S given by (28) and (9), respectively. We have

- (i) The expressions S and $p'(\frac{2\pi}{n})$ have the same sign.

- (ii) assume $\alpha_2 < \beta_{m,w}^-$. Then, for any arbitrary $\bar{\delta}$, we have $p(\frac{\pi}{n}) < 0$.
- (iii) or sufficiently small $\bar{\delta}$, we have $p(\frac{3\pi}{n}) < 0$.

Proof The first part follows from the relation $p'(\frac{2\pi}{n}) = \frac{n}{\sin \frac{2\pi}{n}} S$ (see relation (29)). For the other two parts, note that by Lemma 11 and for odd $1 \leq l \leq n - 1$, we have $p(\frac{l\pi}{n}) = -4 - \frac{2y}{\sin \frac{l\pi}{n}} \sum_{i=0}^{n-1} w_i \sin \frac{il\pi}{n}$. Regarding the case $l = 1$, assumption $\alpha_2 < \beta_{m,w}^-$ implies that $\alpha_2 < 1$ (see Remark 5) and therefore $\alpha_1 < 1$. Thus, $\delta - \delta_0\alpha_1 > 0$, and therefore, $y = y(\alpha_1) = \frac{\delta - \delta_0\alpha_1}{\alpha_1^{2-(m+w)\alpha_1+w}} > 0$. On the other hand, $\sin \frac{i\pi}{n} \geq 0$ for $i = 0, \dots, n - 1$ and so $\sum_{i=0}^{n-1} w_i \sin \frac{i\pi}{n} \geq 0$. This implies $p(\frac{\pi}{n}) < 0$ for any $\bar{\delta}$.

The proof of the last part follows from $\left| \frac{2y}{\sin \frac{3\pi}{n}} \sum_{i=0}^{n-1} w_i \sin \frac{3i\pi}{n} \right| \ll 4$ which holds when $\bar{\delta}$ is small enough.

Proof of parts (iia) and (iib) of Theorem C Since $\alpha_2 < \beta_{m,w}^-$, the spectral gap of L_G is α_2 . It follows from Lemma 11 that $p(\frac{2\pi}{n}) = 0$ for all $\bar{\delta}$. On the other hand, $p(\frac{\pi}{n})$ and $p(\frac{3\pi}{n})$ are both negative for sufficiently small $\bar{\delta}$. Therefore, by intermediate value theorem, the eigenvalue that gets born from α_2 as $\bar{\delta}$ varies is located in the interval (α_2, α_3) if $p'(\frac{2\pi}{n}) > 0$ and is located in (α_1, α_2) if $p'(\frac{2\pi}{n}) < 0$. On the other hand, by part (i) of Lemma 16, we have that $p'(\frac{2\pi}{n})$ and S have the same sign. This proves parts (iia) and (iib) of Theorem C.

Proof of parts (iic), (iid), and (iie) of Theorem C Since $\beta_{m,w}^- < \alpha_2$, the spectral gap of L_G is $\beta_{m,w}^-$. So, we need to see how $\beta_{m,w}^-(\bar{\delta})$ changes as $\bar{\delta}$ varies. By (32), for sufficiently small $\bar{\delta} \neq 0$, we have that $\beta_{m,w}^-(\bar{\delta}) > \beta_{m,w}^-$ if $\frac{(\delta - \delta_0\beta_{m,w}^-)\psi}{\xi} < 0$, and $\beta_{m,w}^-(\bar{\delta}) < \beta_{m,w}^-$ if $\frac{(\delta - \delta_0\beta_{m,w}^-)\psi}{\xi} > 0$. Note that $\delta - \delta_0\beta_{m,w}^- > 0$, since $\delta \geq \delta_0$ and $\beta_{m,w}^- < 1$. Thus, all we need to do is to investigate the sign of $\frac{\psi(\bar{w}, \beta_{m,w}^-)}{\xi(\bar{\delta}, \beta_{m,w}^-)}$.

Note that $\xi(\bar{\delta}, \beta_{m,w}^-)$ and $\xi(0, \beta_{m,w}^-)$ have the same sign provided that $\bar{\delta}$ is sufficiently small and $\xi(0, \beta_{m,w}^-) \neq 0$. Following Lemma 10, $\xi(0, \beta_{m,w}^-) = -2 \sin \theta \tan \frac{n\theta}{2}$, where $\theta = \pi - \cos^{-1}(\frac{\beta_{m,w}^- - 2}{2})$. It is easily seen that $\xi(0, \beta_{m,w}^-) < 0$ if $0 < \beta_{m,w}^- < \alpha_1$, and $\xi(0, \beta_{m,w}^-) > 0$ if $\alpha_1 < \beta_{m,w}^- < \alpha_2$. On the other hand, by Lemma 10,

$$\psi(\bar{w}, \beta_{m,w}^-) = \frac{1}{\cos \frac{n\theta}{2}} \sum_{i=0}^{n-1} w_i \cos\left(\frac{n}{2} - i\right) \theta,$$

where $\theta = \pi - \cos^{-1}(\frac{\beta_{m,w}^- - 2}{2})$. Note that $\cos \frac{n\theta}{2} < 0$ if $\alpha_1 < \beta_{m,w}^- < \alpha_2$, and $\cos \frac{n\theta}{2} > 0$ if $0 < \beta_{m,w}^- < \alpha_1$. Moreover, when $0 < \beta_{m,w}^- < \alpha_1$, we have that $\cos(\frac{n}{2} - i)\theta > 0$ for $i = 0, \dots, n - 1$, and therefore, $\sum_{i=0}^{n-1} w_i \cos(\frac{n}{2} - i)\theta > 0$.

We have

$$\begin{cases} \frac{\psi(\bar{w}, \beta_{m,w}^-)}{\xi(0, \beta_{m,w}^-)} < 0 \text{ if } 0 < \beta_{m,w}^- < \alpha_1, \\ \frac{\psi(\bar{w}, \beta_{m,w}^-)}{\xi(0, \beta_{m,w}^-)} > 0 \text{ if } \alpha_1 < \beta_{m,w}^- < \alpha_2, \text{ and } \sum_{i=0}^{n-1} w_i \cos\left(\frac{n}{2} - i\right)\theta < 0, \\ \frac{\psi(\bar{w}, \beta_{m,w}^-)}{\xi(0, \beta_{m,w}^-)} < 0 \text{ if } \alpha_1 < \beta_{m,w}^- < \alpha_2, \text{ and } \sum_{i=0}^{n-1} w_i \cos\left(\frac{n}{2} - i\right)\theta > 0. \end{cases}$$

This ends the proof of parts (iic), (iid) and (iie) of Theorem C.

Proof of part (ii) of Theorem C Since $\alpha_2 < \beta_{m,w}^-$, we have $\lambda_2(L_G) = \alpha_2$ (see Proposition 1). On the other hand, by Lemma 16, S and $p'(\frac{2\pi}{n})$ have the same sign. If $S < 0$, since $p(\frac{\pi}{n}) < 0$ (see Lemma 16), the intermediate value theorem implies that L_{G_p} has an eigenvalue (p has a root) smaller than α_2 . Denote this eigenvalue by $\lambda(\bar{\delta})$. When the modification is small, this eigenvalue is indeed the spectral gap of L_{G_p} , as discussed in the proof of part (iia). However, for large modification, there is the possibility of the emergence of non-real eigenvalues of L_{G_p} . In such a scenario, there might be complex conjugates eigenvalues of L_{G_p} whose real part decreases and becomes smaller than $\lambda(\bar{\delta})$. This means that the spectral gap is not necessarily a real number; however, since $\lambda(\bar{\delta}) < \alpha_2$, we always have $\text{Re}(\lambda_2(L_{G_p})) < \lambda_2(L_G)$. This proves part (iia) of the theorem.

The proof of part (iia) is similar. For small modifications, as discussed in the proof of part (iib) of the theorem, we have that $\lambda_2(L_{G_p}) = \alpha_2$. In fact, α_2 is an eigenvalue of L_{G_p} for arbitrary $\bar{\delta}$. However, as we discussed above, there is a possibility of the emergence of non-real eigenvalues for L_{G_p} when the modification $\bar{\delta}$ is large. Thus, this might be the case that the real parts of these non-real eigenvalues reduce, and they become the spectral gap of L_{G_p} . In any case, the property $\text{Re}(\lambda_2(L_{G_p})) \leq \lambda_2(L_G)$ always holds. This proves part (iib) of the theorem.

6 Conclusions

This paper investigates how modifying a network affects the Laplacian spectral gap and, in turn, the collective dynamics (synchronization). We considered modifications of three networks with master–slave topology, where the master is a cycle, and the slave is a star. The cycle and star were chosen since they are common motifs in real-world networks. The considered modifications are of arbitrary size and not necessarily (sufficiently) small. Our investigation was based on the spectral analysis of the Laplacian matrices of these networks. Our results are rigorous and accompanied by simulations of networks of coupled Lorenz oscillators that admit our mathematical results.

One particular interest of this paper was a paradoxical scenario known as Braess’s paradox in which improving network connectivity leads to functional failure, such as synchronization loss. We explored and classified such scenarios in these three network models. We have shown that this counter-intuitive scenario in our models is not rare at all. For instance, a critical value exists (proportional to the square root of the size

of the star) for which Braess's paradox happens in models I and II if the cycle size exceeds this value.

Acknowledgements SB, NK, and DE were supported by TUBITAK Grant No. 119F125. DE was supported by the BAGEP Award of the Science Academy, Turkey. TP was supported by a Newton Advanced Fellowship of the Royal Society NAF/R1\180236, by Serrapilheira Institute (Grant No. Serra- 1709-16124), and FAPESP (grant 2013/07375-0). SB and TP acknowledge the support of FAPESP (grant no. 2023/04294-0). SB acknowledges the support of Leverhulme Trust grant RPG-2021-072.

Funding Open access funding provided by the Scientific and Technological Research Council of Türkiye (TÜBİTAK).

Data Availability The datasets generated during and/or analyzed during the current study are available from the authors at reasonable request.

Declarations

Conflict of interest The authors declare that there is no conflict of interest.

Open Access This article is licensed under a Creative Commons Attribution 4.0 International License, which permits use, sharing, adaptation, distribution and reproduction in any medium or format, as long as you give appropriate credit to the original author(s) and the source, provide a link to the Creative Commons licence, and indicate if changes were made. The images or other third party material in this article are included in the article's Creative Commons licence, unless indicated otherwise in a credit line to the material. If material is not included in the article's Creative Commons licence and your intended use is not permitted by statutory regulation or exceeds the permitted use, you will need to obtain permission directly from the copyright holder. To view a copy of this licence, visit <http://creativecommons.org/licenses/by/4.0/>.

A Synchronization of Coupled Rössler Oscillators

We consider the network given model II, with an isolated dynamics $f : \mathbb{R}^3 \rightarrow \mathbb{R}^3$ as the Rössler oscillator, described as

$$\begin{aligned}\dot{x} &= -y - z \\ \dot{y} &= x + 0.2y \\ \dot{z} &= 0.2 + z(x - 5.7).\end{aligned}\tag{A1}$$

Its dynamics is also chaotic like the Lorenz attractor.

A.1 Hinderling Synchronization

At time zero, we consider model II, where the sizes of the cycle and star subgraphs are $n = m = 15$. They are initially connected via a directed link from the cycle to the star subgraph where $w_0 = 1$, as shown in the left upper panel of Fig. 7.

We consider $H = \mathbf{I}$ as the coupling function between oscillators. We randomly choose initial conditions from the uniform distribution over $[0.5, 1)$ and integrate the network until time $t = 1000$ s. In this master–slave configuration, the network converges toward a synchronous motion, where the mean error $\langle E \rangle$ goes to zero. At time $t = 1000$ s, we break the master–slave configuration by adding the cutset

edges $\delta_i = 1$, where $i = 0, 1, \dots, m - 1$. This is represented as the red edges on the right upper panel of Fig. 7. Along with the network modification, we introduce small perturbations to each state randomly selected from the uniform distribution over $[0.01, 0.02)$. As observed, this modification leads to an instability of the synchronous motion.

We can use Theorem B to understand the hindrance of synchronization. We add the cutset edges $\delta_i = 1$, where $i = 0, 1, \dots, m - 1$, which corresponds to the global modification case in Theorem B. We focus to the case b since $\alpha_2 = 0.17, \beta_{15,1}^- = 0.06$. We observe that $\delta < \delta_0 \beta_{15,1}^+$ where $\delta = 15, \delta_0 = 1, \beta_{15,1}^+ = 15.94$. Thus, we can use local modification results from Theorem B. The theorem says $\lambda_2(L_{G_p}) < \lambda_2(L_G)$ since $\alpha_1 < \beta_{15,1}^-$ where $\alpha_1 = 0.04$. In this case, we know that G is more synchronizable than G_p by Definition 1.

A.2 Enhancing Synchronization

Again, we consider model II with $n = 10$ and $m = 20$ along with $H = \mathbf{I}$ as the coupling function as before.

We randomly choose initial conditions from the uniform distribution over $[0.5, 1)$ and integrate the network until time $t = 1000$ s. In this master–slave configuration, the network does not synchronize, as can be observed in the mean synchronization error $\langle E \rangle$. At time $t = 1000$ s, we break the master–slave configuration by adding a cutset and modification edges are $w_0 = 1$ and $\delta_i = 1$, where $i = 0, 1, \dots, m - 1$. This is represented as the red edges on the right upper panel of Fig. 8. After this modification, the synchronous state becomes stable, and the synchronization error converges to zero.

Again, we use Theorem B to deduce the synchronization enhancement. We add the cutset edges $\delta_i = 1$, where $i = 0, 1, \dots, m - 1$, which corresponds to the global

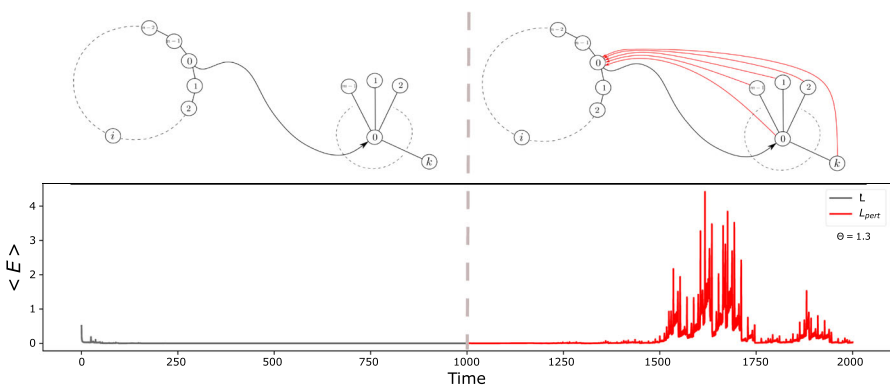


Fig. 7 Hindrance of synchronization due to link addition in networks of coupled Rössler oscillators. The figure shows the synchronization error over time with link addition occurring at time $t = 1000$ s. The sizes of the cycle and star subgraphs are set to $n = 15$ and $m = 15$, and subgraphs are connected via a directed link from the cycle subgraph to the star subgraph where $w_0 = 1$. At $t = 1000$ s, we add the red links to each system with unit weight. After perturbation, the system does not return to synchronization

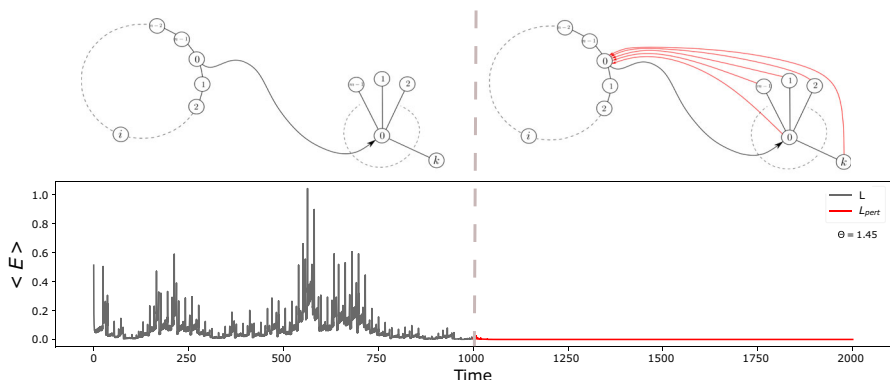


Fig. 8 Enhancement of synchronization due to link addition in a network of coupled Rössler oscillators. The sizes of the cycle and star subgraphs are $n = 10$ and $m = 20$, initially, and subgraphs are connected via a directed link from the cycle to the star where $w_0 = 1$. We integrate the network until time $t = 1000$ s and find the synchronization is unstable. After the red links are added to the system at $t = 1000$ s, the synchronization mean error $\langle E \rangle$ goes to zero, indicating that the modification leads to stable synchronous dynamics

modification case in Theorem B. We focus to the case b since $\alpha_2 = 0.38, \beta_{20,1}^- = 0.05$. We observe that $\delta < \delta_0 \beta_{20,1}^+$ where $\delta = 20, \delta_0 = 1, \beta_{20,1}^+ = 20.95$. Thus, we can use local modification results. The theorem says $\lambda_2(L_G) < \lambda_2(L_{G_p})$ since $\beta_{20,1}^- < \alpha_1$ where $\alpha_1 = 0.1$. In this case, we know that G_p is more synchronizable than G by Definition 1.

B Technical Lemmas

Lemma B.17 Consider the block matrix $\begin{pmatrix} A & B \\ C & D \end{pmatrix}$ and assume D is invertible. Define $E := A - BD^{-1}C$. Then,

(i) $\det \begin{pmatrix} A & B \\ C & D \end{pmatrix} = \det(D) \times \det(E)$.

(ii) Assume E is invertible. Then, $\begin{pmatrix} A & B \\ C & D \end{pmatrix}^{-1} = \begin{pmatrix} E^{-1} & -E^{-1}BD^{-1} \\ -D^{-1}CE^{-1} & D^{-1} + D^{-1}CE^{-1}BD^{-1} \end{pmatrix}$.

Proof See, e.g., Meyer (2000).

Lemma B.2 For $m \geq 4$, let X_0, X_1, \dots, X_{m-1} be real-valued functions defined on a subset of \mathbb{R} , and consider the $m \times m$ matrix

$$M = M(\lambda) = \left(\begin{array}{c|cccc} m - \lambda + X_0(\lambda) & -1 & + X_1(\lambda) & -1 & + X_2(\lambda) & \dots & -1 & + X_{m-1}(\lambda) \\ \mathbf{1}_{m-1} & & & & & & (1 - \lambda) \mathbf{I} & \end{array} \right).$$

Let $\lambda_0 \in \mathbb{R}$, and assume that all the functions X_i are defined at λ_0 .

(i) There exists $0 \neq v \in \mathbb{R}^m$ such that $M(\lambda_0)v = 0$ if and only if $\lambda_0 = 1$ or $\lambda = \lambda_0$ satisfies

$$\lambda^2 - [1 + m + X_0(\lambda)]\lambda + 1 + \sum_{i=0}^{m-1} X_i(\lambda) = 0. \tag{B2}$$

- (ii) Assume that there exists $1 \leq i \leq m - 1$ such that $X_i(1) \neq 1$. Then, the vector subspace $E^{\text{right}} \subset \mathbb{R}^m$ (resp. $E^{\text{left}} \subset \mathbb{R}^m$) of all the solutions v of the equation $M(1)v = 0$ (resp. $v^\top M(1) = 0$) has $m - 2$ dimensions.
- (iii) Let $v = (v_0, v_1, \dots, v_{m-1}) \in \mathbb{R}^m$. Then, any $v \in E^{\text{right}}$ satisfies the property $v_0 = 0$. Moreover, if there exists $1 \leq i \leq m - 1$ such that $X_i(1) \neq 1$, then any $v \in E^{\text{left}}$ satisfies the property $v_0 = 0$ too.

Proof For $v = (v_0, v_1, \dots, v_{m-1}) \in \mathbb{R}^m$, we have $M(\lambda)v = 0$ if and only if

$$[m - \lambda + X_0(\lambda)]v_0 + \sum_{i=1}^{m-1} [-1 + X_i(\lambda)]v_i = 0, \quad \text{and} \quad (\text{B3})$$

$$v_0 + (1 - \lambda)v_i = 0, \quad \text{for all } 1 \leq i \leq m - 1. \quad (\text{B4})$$

This implies that for $\lambda = 1$, the equation $M(1)v = 0$ has a solution v if and only if $v \in E^{\text{right}}$ for

$$E^{\text{right}} := \{v \in \mathbb{R}^m \mid v_0 = 0 \text{ and } \langle (v_1, v_2, \dots, v_{m-1}), (X_1(1) - 1, \dots, X_{m-1}(1) - 1) \rangle = 0\}, \quad (\text{B5})$$

where $\langle \cdot, \cdot \rangle$ is the standard Euclidean inner product in \mathbb{R}^{m-1} .

If $M(1)v = 0$, for $\lambda \neq 1$, has a solution v , then it follows from (B4) that $v_0 \neq 0$ and $v_i = \frac{v_0}{1-\lambda}$, for all $1 \leq i \leq m - 1$. Substituting this into (B3) and multiplying the derived equation by $1 - \lambda$ give (B2). This proves part (i).

Part (ii) follows from (B5). To prove part (iii), let $v \in E^{\text{left}}$. By $v^\top M(1) = 0$, we have that if there exists $1 \leq i \leq m - 1$ such that $X_i(1) \neq 1$, then $v_0 = 0$ and $v_1 + v_2 + \dots + v_{m-1} = 0$. The set of all v s satisfying these properties is a $(m - 2)$ -dimensional subspace of \mathbb{R}^m . This finishes the proof of the lemma.

References

- Aguiar, M.A.D., Dias, A., Field, M.: Feedforward networks: adaptation, feedback, and synchrony. *J. Nonlinear Sci.* **29**(3), 1129–1164 (2019)
- Alexander, G.E., DeLong, M.R., Strick, P.L.: Parallel organization of functionally segregated circuits linking basal ganglia and cortex. *Annu. Rev. Neurosci.* **9**(1), 357–381 (1986)
- Ben-Yishai, R., Hansel, D., Sompolinsky, H.: Traveling waves and the processing of weakly tuned inputs in a cortical network module. *J. Comput. Neurosci.* **4**, 57–77 (1997)
- Biyikoglu, T., Leydold, J., Stadler, P.F.: *Laplacian Eigenvectors of Graphs: Perron-Frobenius and Faber-Krahn Type Theorems*. Springer, Cham (2007)
- Bonifazi, P., Goldin, M., Picardo, M.A., Jorquera, I., Cattani, A., Bianconi, G., Represa, A., Ben-Ari, Y., Cossart, R.: Gabaergic hub neurons orchestrate synchrony in developing hippocampal networks. *Science* **326**(5958), 1419–1424 (2009)
- Brouwer, A.E., Haemers, W.H.: *Spectra of Graphs*. Springer, New York (2011)
- Chung, F.R.: *Spectral Graph Theory*, vol. 92. American Mathematical Society, Providence (1997)
- Corder, R.M., Bian, Z., Pereira, T., Montalbán, A.: Emergence of chaotic cluster synchronization in heterogeneous networks. *Chaos Interdiscip. J. Nonlinear Sci.* **33**(9), 091103 (2023)
- Eguiluz, V.M., Chialvo, D.R., Cecchi, G.A., Baliki, M., Apkarian, A.V.S.: Scale-free brain functional networks. *Phys. Rev. Lett.* **94**(1), 018102 (2005)
- Eldan, R., Rácz, M.Z., Schramm, T.: Braess's paradox for the spectral gap in random graphs and delocalization of eigenvectors. *Random Struct. Algorithms* **50**(4), 584–611 (2017)

- Ermentrout, B., Terman, D.H.: *Mathematical Foundations of Neuroscience*, vol. 35. Springer, New York (2010)
- Eroglu, D., Lamb, J.S.W., Pereira, T.: Synchronisation of chaos and its applications. *Contemp. Phys.* **58**(3), 207–243 (2017)
- Field, M.: Heteroclinic networks in homogeneous and heterogeneous identical cell systems. *J. Nonlinear Sci.* **25**(3), 779–813 (2015)
- Hart, J.D., Pade, J.P., Pereira, T., Murphy, T.E., Roy, R.: Adding connections can hinder network synchronization of time-delayed oscillators. *Phys. Rev. E* **92**(2), 022804 (2015)
- Horn, R., Johnson, C.R.: *Matrix Analysis*. Cambridge University Press, New York (2012)
- Hu, G.Y., O’Connell, R.F.: Analytical inversion of symmetric tridiagonal matrices. *J. Phys. A Math. Gen.* **29**(7), 1511 (1996)
- Kantner, M., Yanchuk, S.: Bifurcation analysis of delay-induced patterns in a ring of Hodgkin-Huxley neurons. *Philos. Trans. R. Soc. A Math. Phys. Eng. Sci.* **371**(1999), 20120470 (2013)
- Kashtan, N., Alon, U.: Spontaneous evolution of modularity and network motifs. *Proc. Natl. Acad. Sci.* **102**(39), 13773–13778 (2005)
- Loudop, P., Tchitnga, R., Fagundes, F.F., Kountchou, M., Tamba, V.K., Pando, C.L., Cerdeira, H.A.: Extreme multistability in a Josephson-junction-based circuit. *Phys. Rev. E* **99**(4), 042208 (2019)
- Ma’ayan, A., Cecchi, G.A., Wagner, J., Rao, A.R., Iyengar, R., Stolovitzky, G.: Ordered cyclic motifs contribute to dynamic stability in biological and engineered networks. *Proc. Natl. Acad. Sci.* **105**(49), 19235–19240 (2008)
- Manik, D., Timme, M., Witthaut, D.: Cycle flows and multistability in oscillatory networks. *Chaos Interdiscip. J. Nonlinear Sci.* **27**(8), 083123 (2017)
- Mersing, D., Tyler, S.A., Ponboonjaroenchai, B., Tinsley, M.R., Showalter, K.: Novel modes of synchronization in star networks of coupled chemical oscillators. *Chaos Interdiscip. J. Nonlinear Sci.* **31**(9), 093127 (2021)
- Meyer, C.D.: *Matrix Analysis and Applied Linear Algebra*, vol. 71. SIAM, Philadelphia (2000)
- Milanese, A., Sun, J., Nishikawa, T.: Approximating spectral impact of structural perturbations in large networks. *Phys. Rev. E* **81**(4), 046112 (2010)
- Mohar, B.: Some applications of Laplace eigenvalues of graphs. In: *Graph Symmetry: Algebraic Methods and Applications*, pp. 225–275. Springer (1997)
- Muni, S.S., Provata, A.: Chimera states in ring-star network of Chua circuits. *Nonlinear Dyn.* **101**(4), 2509–2521 (2020)
- Newman, M.: *Networks*, pp. 17–99. Oxford University Press, Oxford (2018)
- Nishikawa, T., Motter, A.E.: Network synchronization landscape reveals compensatory structures, quantization, and the positive effect of negative interactions. *Proc. Natl. Acad. Sci.* **107**(23), 10342–10347 (2010)
- Pade, J.P., Pereira, T.: Improving network structure can lead to functional failures. *Sci. Rep.* **5**(1), 1–6 (2015)
- Pereira, T., Eldering, J., Rasmussen, M., Veneziani, A.: Towards a theory for diffusive coupling functions allowing persistent synchronization. *Nonlinearity* **27**(3), 501–525 (2014)
- Pereira, T., Van Strien, S., Tanzi, M.: Heterogeneously coupled maps: hub dynamics and emergence across connectivity layers. *J. Eur. Math. Soc.* **22**(7), 2183–2252 (2020)
- Poignard, C., Pade, J.P., Pereira, T.: The effects of structural perturbations on the synchronizability of diffusive networks. *J. Nonlinear Sci.* **29**(5), 1919–1942 (2019)
- Prasad, A., Dhamala, M., Adhikari, B.M., Ramaswamy, R.: Amplitude death in nonlinear oscillators with nonlinear coupling. *Phys. Rev. E* **81**(2), 027201 (2010)
- Tönjes, R., Fiore, C.E., Pereira, T.: Coherence resonance in influencer networks. *Nat. Commun.* **12**(1), 72 (2021)
- Veerman, J.J.P., Lyons, R.: A primer on Laplacian dynamics in directed graphs. *Nonlinear Phenomena in Complex Systems* **23**, 196–206 (2020)
- Vlasov, V., Zou, Y., Pereira, T.: Explosive synchronization is discontinuous. *Phys. Rev. E* **92**(1), 012904 (2015)